MATCH
Communications in Mathematical and in Computer Chemistry

MATCH Commun. Math. Comput. Chem. **57** (2007) 5-48

ISSN 0340 - 6253

Mandalas and Fujita's Proligand Method. A Novel Way of Stereochemistry Through the Concepts of Coset Representations and Sphericities (Part 4)

Shinsaku Fujita
Department of Chemistry and Materials Technology,
Kyoto Institute of Technology,
Matsugasaki, Sakyoku, Kyoto 606-8585, Japan
E-mail: fujitas@chem.kit.ac.jp

(Received March 23, 2006)

Abstract

Fujita's proligand method, which was originally formulated by using the symmetrical properties of cyclic subgroups (Fujita, S. (2005) *Theor. Chem. Acc.*, **113** 73–79, 80–86), has been alternatively formulated in terms of the concept of mandalas proposed in Part 2 of this series (Fujita, S. (2006) *MATCH Commun. Math. Comput. Chem.*, **55**, 5–38). A set of assemblies of **K**-symmetry in a mandala of **G**-symmetry has been characterized by the left coset representation **G**(/**K**), where achiral assemblage and chiral assemblage have been discussed in terms of the chirality/achirality of the group **K**. Each **K**-assembled mandala has been shown to correspond to one stereoisomer of **K**-symmetry, i.e., an achiral molecule or a pair of enantiomers. The alternative formulation of Fujita's proligand method has been accomplished by comparing the number of fixed assemblies per stereoisomer with the number of fixed assemblies per permutation. Thereby, stereoisomers can be enumerated in an itemized fashion, i.e., the numbers of achiral plus chiral stereoisomers, of achiral stereoisomers, and of chiral stereoisomers. Deficiency of Pólya's theorem in stereoisomer

enumeration and merits of Fujita's proligand method have been demonstrated by using allenes and prismanes as examples.

1 Introduction

In Part 1 of this series [1], a *regular body* has been discussed as a diagrammatical expression for characterizing intramolecular stereochemistry. In Part 2 of this series [2], a *mandala* (a nested regular body) has been discussed as a diagrammatical expression for characterizing stereoisomerism (i.e., intermolecular stereochemistry). These two types of diagrammatical expressions can be treated commonly because they have mathematically equivalent properties. In particular, the mathematical equivalence between the segmentation of a regular body and the assemblage of a mandala has been demonstrated diagrammatically. In Part 3 [3], the close relationship between the two operations (the segmentation and the assemblage) has been diagrammatically examined so as to provide a succinct basis of stereoisomer enumeration, which has once been formulated as Fujita's USCI (unit-subduced-cycle-index) approach in a more algebraic fashion [4]. Throughout this series [1, 2, 3] along with the original version of the USCI approach [4], the concept of sphericity (the sphericities of orbits governed by coset representations) has been emphasized as a key to characterize stereoisomers as three-dimensional objects having inner structure (e.g., chirality/achirality of ligands).

On the other hand, Pólya's theorem [5, 6], which has been widely used in chemical combinatorics [7, 8, 9], has failed in characterizing stereoisomers as three-dimensional objects having inner structure. This failure has not been pointed out until recently and turns out to have been demonstrated only implicitly by combining several references [10, 11]. For example, Pólya et al. [12] have discussed stereoisomer enumeration of prismane derivatives by using the $\mathbf{D}_3$ permutation group as well as the permutation group corresponding to $\mathbf{D}_{3h}$-point group, where only atoms with no inner structure have been considered as substituents on the vertices of the prismane skeleton. Although their treatment is correct in the context of their book [12], it would give stereochemically inconsistent results if inner structure (e.g., ligands p of one chirality and other ligands $\overline{\mathrm{p}}$ of the opposite chirality) is taken into consideration. In particular, their treatment is incapable of discriminating properly between asymmetric cases (or enantiomeric relationship) and pseudoasymmetric cases (or diastereomeric relationship). The CI (cycle-index) method described in Part 3 [3] and in other references [13, 14] has clarified that the reason of the incapability is that Pólya's theorem does not involve the sphericity concept from a viewpoint brought about by the USCI approach.

To avoid the drawback of Pólya's theorem, we have proposed *the proligand method* [15, 16, 17], which is capable of characterizing and enumerating stereoisomers as three-dimensional objects having inner structure. For this proposal, the sphericity concept for the USCI approach, which was originally formulated as *sphericity of orbits*, has been modified into a new concept *sphericities of cycles* [15, 16, 17] through an intermediate concept "sphericities of orbits for cyclic subgroups" [18, 19, 20, 21]. Even though the USCI approach has become very accessible by means of the diagrammatical approach of the present series, a more direct modification without such an intermediate concept would be desirable for readers who are not acquainted with the USCI approach to comprehend the new concept *sphericities of cycles*.

In the present paper (Part 4), the concept of mandala introduced in Part 2 will be studied in another way to introduce directly the sphericity concept in stereoisomer enumeration. Thereby, an alternative formulation of the proligand method will be demonstrated.

2 Right and Left Cosets

2.1 Reference Numbering and Inverse Numbering

In Part 1 to Part 3 [1, 2, 3], we have used the symbol $\mathbf{G}(/\mathbf{H})$ for representing coset representations (CR) so that we have not discriminated between right coset representations (RCR) and left coset representations (LCR). To go on further and detailed discussions, we shall discriminate between them. Thus, let us use the symbol $(\mathbf{H}\backslash)\mathbf{G}$ for representing the RCR and the symbol $\mathbf{G}(/\mathbf{H})$ for representing the LCR. It follows that the positions of regular bodies etc. discussed in Part 1 are considered to be controlled by the RCR $(\mathbf{H}\backslash)\mathbf{G}$, which is correlated to permutations on a set of right cosets $\mathbf{H}\backslash\mathbf{G}$.[1] On the other hand, the transformulas of mandalas etc. discussed in Part 2 are considered to be controlled by the LCR $\mathbf{G}(/\mathbf{H})$, which is correlated to permutations on a set of right cosets $\mathbf{G}/\mathbf{H}$.

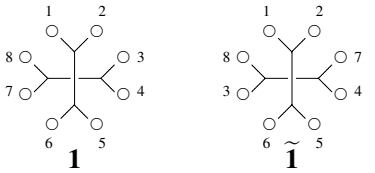

Figure 1: Regular bodies with a reference numbering (**1**) and with the inverse numbering ($\widetilde{\mathbf{1}}$).

According to eq. 73 of Part 1, the symmetry operations of $\mathbf{D}_{2d}$ corresponds to the eight positions of a regular body of $\mathbf{D}_{2d}$ (**1**) so as to give a reference numbering as follows:

$$\mathbf{D}_{2d} = \mathbf{C}_1\backslash\mathbf{D}_{2d} = \{\underbrace{I}_{1}, \underbrace{\sigma_{d(1)}}_{2}, \underbrace{S_4}_{3}, \underbrace{C_{2(1)}}_{4}, \underbrace{C_{2(3)}}_{5}, \underbrace{\sigma_{d(2)}}_{6}, \underbrace{S_4^3}_{7}, \underbrace{C_{2(2)}}_{8}\}. \tag{1}$$

Thus, the group $\mathbf{D}_{2d}$ as an ordered set is recognized to be an ordered set $\mathbf{C}_1\backslash\mathbf{D}_{2d}$, which is regarded as an extreme case of an ordered set of right cosets. This means that the set $\mathbf{C}_1\backslash\mathbf{D}_{2d}$ and the corresponding set of positions in the regular body (**1**) are both governed by the RCR $(\mathbf{C}_1\backslash)\mathbf{D}_{2d}$. The concrete form of the RCR $(\mathbf{C}_1\backslash)\mathbf{D}_{2d}$ has been shown in eqs. 14–21 of Part 1, which have been obtained diagrammatically.

By recognizing the $\mathbf{C}_1\backslash\mathbf{D}_{2d}$-set (eq. 1), we are able to consider another ordered set $\mathbf{D}_{2d}/\mathbf{C}_1$, where any $g \in \mathbf{D}_{2d}$ is replaced by g^{-1} as follows:

$$\begin{aligned}\mathbf{D}_{2d}/\mathbf{C}_1 &= \{\underbrace{I^{-1}}_{1}, \underbrace{\sigma_{d(1)}^{-1}}_{2}, \underbrace{S_4^{-1}}_{3}, \underbrace{C_{2(1)}^{-1}}_{4}, \underbrace{C_{2(3)}^{-1}}_{5}, \underbrace{\sigma_{d(2)}^{-1}}_{6}, \underbrace{S_4^{-3}}_{7}, \underbrace{C_{2(2)}^{-1}}_{8}\} \\ &= \{\underbrace{I}_{1}, \underbrace{\sigma_{d(1)}}_{2}, \underbrace{S_4^3}_{3}, \underbrace{C_{2(1)}}_{4}, \underbrace{C_{2(3)}}_{5}, \underbrace{\sigma_{d(2)}}_{6}, \underbrace{S_4}_{7}, \underbrace{C_{2(2)}}_{8}\}\end{aligned} \tag{2}$$

which gives the corresponding inverse numbering ($\tilde{\mathbf{1}}$) as shown in Fig. 1. Thus, the group $\mathbf{D}_{2d}$ is alternatively recognized to be an ordered set $\mathbf{D}_{2d}/\mathbf{C}_1$, which is regarded as an extreme case of

[1] Equation 75 of Part 1 should be replaced by the corresponding right coset decomposition, i.e., $\mathbf{D}_{2d} = \mathbf{C}_s I + \mathbf{C}_s C_{2(3)} + \mathbf{C}_s C_{2(1)} + \mathbf{C}_s C_{2(2)}$.

second operation \ first operation		1 I	2 $\sigma_{d(1)}$	3 S_4	4 $C_{2(1)}$	5 $C_{2(3)}$	6 $\sigma_{d(2)}$	7 S_4^3	8 $C_{2(2)}$
1	I	1	2	3	4	5	6	7	8
2	$\sigma_{d(1)}$	2	1	4	3	6	5	8	7
3	S_4	3	8	5	2	7	4	1	6
4	$C_{2(1)}$	4	7	6	1	8	3	2	5
5	$C_{2(3)}$	5	6	7	8	1	2	3	4
6	$\sigma_{d(2)}$	6	5	8	7	2	1	4	3
7	S_4^3	7	4	1	6	3	8	5	2
8	$C_{2(2)}$	8	3	2	5	4	7	6	1

Figure 2: Multiplication table of $\mathbf{D}_{2d}$

an ordered set of left cosets. The eight transformulas of a mandala (as a base body) obey such an inverse numbering, as discussed in Part 2.

The symmetrical behavior of the regular bodies (**1** and $\tilde{\mathbf{1}}$) are correlated to the multiplication table shown in Fig. 2, which adopts the reference numbering shown in eq. 1. The concrete permutations of the RCR $(\mathbf{C}_1\backslash)\mathbf{D}_{2d}$ for **1** (eqs. 14–21 of Part 1) are obtained by collecting every columns of Fig. 2. On the other hand, by collecting every rows of Fig. 2, we can construct the LCR $\mathbf{D}_{2d}(/\mathbf{C}_1)$.

2.2 Effect of Segmentation

The effect of $\mathbf{C}_s$-segmentation is shown in Fig. 3, where the resulting four $\mathbf{C}_s$-segments are equivalent under the action of $\mathbf{D}_{2d}$. The process of segmentation is interpreted as the superposition of a segmentation pattern of $\mathbf{C}_s$ (shown by oval boxes in **2**) onto the regular body with the reference numbering (**1**). Thereby, the corresponding segmented regular body (**2**) shown in Fig. 3 is explained by the following set of right cosets:

$$\begin{aligned}\mathbf{C}_s\backslash\mathbf{D}_{2d} &= \left\{\underbrace{\mathbf{C}_s I}_{1},\underbrace{\mathbf{C}_s S_4}_{2},\underbrace{\mathbf{C}_s C_{2(3)}}_{3},\underbrace{\mathbf{C}_s S_4^3}_{4}\right\}\\ &= \left\{\underbrace{\{1,2\}}_{1},\underbrace{\{3,4\}}_{2},\underbrace{\{5,6\}}_{3},\underbrace{\{7,8\}}_{4}\right\},\end{aligned} \tag{3}$$

where the right cosets are numbered sequentially. The set of four $\mathbf{C}_s$-segments, i.e., $\mathcal{A} = \{\mathcal{A}_1,\mathcal{A}_2,\mathcal{A}_3,\mathcal{A}_4\}$, constructs an orbit governed by the RCR $(\mathbf{C}_s\backslash)\mathbf{D}_{2d}$ because of the correspondence between $\mathbf{C}_s\backslash\mathbf{D}_{2d}$ (eq. 3) and $\mathcal{A}$ of **2**.

By examining the action of all of the operation of $\mathbf{D}_{2d}$ on the set of four $\mathbf{C}_s$-segments ($\mathcal{A} = \{\mathcal{A}_1,\mathcal{A}_2,\mathcal{A}_3,\mathcal{A}_4\}$) diagrammatically or by examining the corresponding action on the set of cosets ($\mathbf{C}_s\backslash\mathbf{D}_{2d}$ shown in eq. 3) algebraically, the concrete form of the RCR $(\mathbf{C}_s\backslash)\mathbf{D}_{2d}$ is

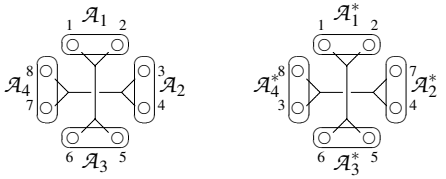

Figure 3: Segmented regular bodies with a reference numbering (**2**) and with the inverse numbering ($\widetilde{\mathbf{2}}$). The four oval boxes in each segmented regular body are regarded as constructing a $\mathbf{C}_s$-segmentation pattern.

calculated as follows:

$$I \sim \begin{pmatrix} 1 & 2 & 3 & 4 \\ 1 & 2 & 3 & 4 \end{pmatrix} = (1)(2)(3)(4) \tag{4}$$

$$C_{2(1)} \sim \begin{pmatrix} 1 & 2 & 3 & 4 \\ 2 & 1 & 4 & 3 \end{pmatrix} = (1\,2)(3\,4) \tag{5}$$

$$C_{2(2)} \sim \begin{pmatrix} 1 & 2 & 3 & 4 \\ 4 & 3 & 2 & 1 \end{pmatrix} = (1\,4)(2\,3) \tag{6}$$

$$C_{2(3)} \sim \begin{pmatrix} 1 & 2 & 3 & 4 \\ 3 & 4 & 1 & 2 \end{pmatrix} = (1\,3)(2\,4) \tag{7}$$

$$\sigma_{d(1)} \sim \begin{pmatrix} 1 & 2 & 3 & 4 \\ \overline{1} & \overline{4} & \overline{3} & \overline{2} \end{pmatrix} = \overline{(1)(3)(2\,4)} \tag{8}$$

$$S_4 \sim \begin{pmatrix} 1 & 2 & 3 & 4 \\ \overline{2} & \overline{3} & \overline{4} & \overline{1} \end{pmatrix} = \overline{(1\,2\,3\,4)} \tag{9}$$

$$S_4^3 \sim \begin{pmatrix} 1 & 2 & 3 & 4 \\ \overline{4} & \overline{1} & \overline{2} & \overline{3} \end{pmatrix} = \overline{(1\,4\,3\,2)} \tag{10}$$

$$\sigma_{d(2)} \sim \begin{pmatrix} 1 & 2 & 3 & 4 \\ \overline{3} & \overline{2} & \overline{1} & \overline{4} \end{pmatrix} = \overline{(1\,3)(2)(4)}, \tag{11}$$

where an overbar represents the inversion of one chirality into an opposite chirality. For the sake of convenience, these permutations are classified into four proper rotations without an overbar (the upper four) and four improper rotations with an overbar (the bottom four). These permutations of $(\mathbf{C}_s\backslash)\mathbf{D}_{2d}$ control the symmetrical behavior of the four positions of the allene skeleton, where each of the segments of **2** is regarded as a position of the allene skeleton. In other words, the RCR $(\mathbf{C}_s\backslash)\mathbf{D}_{2d}$ governs the orbit (equivalence class) of the four positions in the allene skeleton.

On the other hand, the $\mathbf{C}_s$-segmentation pattern is superposed onto the regular body with the inverse numbering ($\widetilde{\mathbf{1}}$) so as to generate the corresponding segmented regular body ($\widetilde{\mathbf{2}}$), as shown in Fig. 3. The result is explained by the following set of left cosets:

$$\mathbf{D}_{2d}/\mathbf{C}_s = \left\{ \underbrace{I\mathbf{C}_s}_{1}, \underbrace{S_4^{-1}\mathbf{C}_s}_{2}, \underbrace{C_{2(3)}^{-1}\mathbf{C}_s}_{3}, \underbrace{S_4^{-3}\mathbf{C}_s}_{4} \right\}$$

$$= \left\{ \underbrace{I\mathbf{C}_s}_{1}, \underbrace{S_4^3\mathbf{C}_s}_{2}, \underbrace{C_{2(3)}\mathbf{C}_s}_{3}, \underbrace{S_4\mathbf{C}_s}_{4} \right\}$$

$$= \left\{ \underbrace{\{1,2\}}_{1}, \underbrace{\{7,4\}}_{2}, \underbrace{\{5,6\}}_{3}, \underbrace{\{3,8\}}_{4} \right\} \tag{12}$$

The set of four $\mathbf{C}_s$-segments, i.e., $\mathcal{A}^* = \{\mathcal{A}_1^*, \mathcal{A}_2^*, \mathcal{A}_3^*, \mathcal{A}_4^*\}$, constructs an orbit governed by the LCR $\mathbf{D}_{2d}(/\mathbf{C}_s)$ because of the correspondence between $\mathbf{D}_{2d}/\mathbf{C}_s$ (eq. 12) and $\mathcal{A}^*$ of $\widetilde{\mathbf{2}}$.

By examining the action of all of the operation of $\mathbf{D}_{2d}$ on the set of four $\mathbf{C}_s$-segments ($\mathcal{A}^* = \{\mathcal{A}_1^*, \mathcal{A}_2^*, \mathcal{A}_3^*, \mathcal{A}_4^*\}$) diagrammatically or by examining the corresponding action on the set of cosets ($\mathbf{D}_{2d}/\mathbf{C}_s$ shown in eq. 12) algebraically, the concrete form of the LCR $\mathbf{D}_{2d}(/\mathbf{C}_s)$ is calculated as follows:

$$I \sim \begin{pmatrix} 1 & 2 & 3 & 4 \\ 1 & 2 & 3 & 4 \end{pmatrix} = (1)(2)(3)(4) \tag{13}$$

$$C_{2(1)} \sim \begin{pmatrix} 1 & 2 & 3 & 4 \\ 2 & 1 & 4 & 3 \end{pmatrix} = (1\,2)(3\,4) \tag{14}$$

$$C_{2(2)} \sim \begin{pmatrix} 1 & 2 & 3 & 4 \\ 4 & 3 & 2 & 1 \end{pmatrix} = (1\,4)(2\,3) \tag{15}$$

$$C_{2(3)} \sim \begin{pmatrix} 1 & 2 & 3 & 4 \\ 3 & 4 & 1 & 2 \end{pmatrix} = (1\,3)(2\,4) \tag{16}$$

$$\sigma_{d(1)} \sim \begin{pmatrix} 1 & 2 & 3 & 4 \\ \bar{1} & \bar{4} & \bar{3} & \bar{2} \end{pmatrix} = \overline{(1)(3)(2\,4)} \tag{17}$$

$$S_4 \sim \begin{pmatrix} 1 & 2 & 3 & 4 \\ \bar{4} & \bar{1} & \bar{2} & \bar{3} \end{pmatrix} = \overline{(1\,4\,3\,2)} \tag{18}$$

$$S_4^3 \sim \begin{pmatrix} 1 & 2 & 3 & 4 \\ \bar{2} & \bar{3} & \bar{4} & \bar{1} \end{pmatrix} = \overline{(1\,2\,3\,4)} \tag{19}$$

$$\sigma_{d(2)} \sim \begin{pmatrix} 1 & 2 & 3 & 4 \\ \bar{3} & \bar{2} & \bar{1} & \bar{4} \end{pmatrix} = \overline{(1\,3)(2)(4)}, \tag{20}$$

The relationship between $\mathbf{2}$ and $\widetilde{\mathbf{2}}$ can be easily extended into general cases. Let us select $h \in \mathbf{H}$, where the $\mathbf{H}$ is a subgroup of $\mathbf{G}$. Among the right cosets contained in $\mathbf{H}\backslash\mathbf{G}$, a right coset $\mathbf{H}g_i$ is taken into consideration. Then, for $\forall hg_i \in \mathbf{H}g_i$, the inverse is obtained as follows: $(hg_i)^{-1} = g_i^{-1}h^{-1} \in g_i^{-1}\mathbf{H}$. It follows that any element of the right coset $\mathbf{H}g_i$ corresponds to an element of the left coset $g_i^{-1}\mathbf{H}$ in one-to-one fashion. This means that a common $\mathbf{H}$-segmentation pattern operated on regular bodies with a reference numbering and with its inverse numbering gives diagrams of the same appearance.

2.3 Effect of Subduction

The subduction of regular representations has been discussed diagrammatically in Part 1 (cf. eq. 58) and algebraically in Section 7.1 of Fujita's book [4]. We here adopt a subduction pattern that represents the division of the positions of a regular body during the subduction of a regular representation.

For example, select S_4 from $\mathbf{C}_1\backslash\mathbf{D}_{2d}$ (eq. 1). The element S_4 is transformed into $S_4 I = S_4$, $S_4\sigma_{d(1)} = C_{2(2)}$ during the subduction by $\mathbf{C}_s$. Thereby the set $\{S_4, C_{2(2)}\} = \{3,8\}$ is generated.

This procedure repeated to cover the set $\mathbf{C}_1\backslash\mathbf{D}_{2d}$ so as to generate the following division:

$$\mathbf{C}_1\backslash\mathbf{D}_{2d} \xrightarrow{\downarrow\mathbf{C}_s} \{\underbrace{I}_{1},\underbrace{\sigma_{d(1)}}_{2}\}+\{\underbrace{S_4}_{3},\underbrace{C_{2(2)}}_{8}\}+\{\underbrace{C_{2(1)}}_{4},\underbrace{S_4^3}_{7}\}+\{\underbrace{C_{2(3)}}_{5},\underbrace{\sigma_{d(2)}}_{6}\}. \tag{21}$$

If the resulting set $\{S_4, C_{2(2)}\} = \{3, 8\}$ is regarded as corresponding to $\{I, \sigma_{d(1)}\}$ by omitting S_4, it can be recognized to be governed by the right regular representation $(\mathbf{C}_1\backslash)\mathbf{C}_s$. The division shown in eq. 21 is illustrated by the subduced regular body (**3**) as shown in Fig. 4 and summarized as the subduction as follows:

$$(\mathbf{C}_1\backslash)\mathbf{D}_{2d} \downarrow \mathbf{C}_s = 4(\mathbf{C}_1\backslash)\mathbf{C}_s, \tag{22}$$

which has been reported as eq. 57 of Part 1.

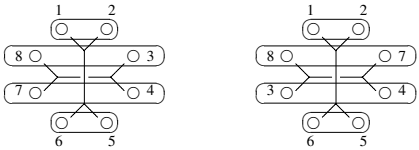

3 $\quad\quad$ $\widetilde{\mathbf{3}}$

Figure 4: Subduced regular bodies with a reference numbering (**3**) and with the inverse numbering ($\widetilde{\mathbf{3}}$).

The set $\{S_4, C_{2(2)}\} = \{3, 8\}$ is alternatively regarded as a left coset $S_4\mathbf{C}_s$. From this point of view, eq. 21 for the division of the set $\mathbf{C}_1\backslash\mathbf{D}_{2d}$ by $\mathbf{C}_s$ is the same thing as a left coset decomposition of $\mathbf{D}_{2d}$ by $\mathbf{C}_s$ in accord with $\mathbf{D}_{2d}/\mathbf{C}_s$ (eq. 12). In other words, the subduction of the RRR $(\mathbf{C}_1\backslash)\mathbf{D}_{2d} \downarrow \mathbf{C}_s$ (**3**) is correlated diagrammatically to the LCR $\mathbf{D}_{2d}(/\mathbf{C}_s)$ ($\widetilde{\mathbf{2}}$).

On the same line, eq. 23 corresponding to eq. 22 is obtained:

$$\mathbf{D}_{2d}(/\mathbf{C}_1) \downarrow \mathbf{C}_s = 4\mathbf{C}_s(/\mathbf{C}_1) \tag{23}$$

Moreover, the subduction of the LRR $\mathbf{D}_{2d}(/\mathbf{C}_1) \downarrow \mathbf{C}_s$ ($\widetilde{\mathbf{3}}$) is correlated diagrammatically to the RCR $(\mathbf{C}_s\backslash)\mathbf{D}_{2d}$ (**2**).

3 Mandalas

A mandala proposed in Part 2 of this series [2] is a model for representing the symmetry of an achiral stereoisomer or a pair of enantiomers. By considering the absence or presence of assemblage, mandalas are classified into non-assembled mandalas and assembled ones. The **G**-symmetry of a regular body is maintained in a non-assembled mandala, which models a starting skeleton. On the other hand, a subgroup **K** of the group **G** appears as **K**-assemblies in an assembled mandala, which is regarded as a model of a **K**-molecule derived from the **G**-skeleton. In this section, the number of fixed points[2] (assemblies) on the action of **G** is shown to be equal to $|\mathbf{G}|$ with and without assemblage (i.e., regardless of **K**).

[2]The term "point" is used in an abstract fashion. Concretely speaking, the term "assembly" should be used here in the context concerning a mandala. The term "point" refers to the term "position", when a regular body or a skeleton is taken into consideration.

3.1 Non-Assembled Mandalas

Without Segmentation According to Part 2 [2], a *mandala* is defined as a nested regular body, where a transformula derived from a regular body (named a *corona body*) is placed on a vertex of another hypothetical regular body (named *a base body*), as shown in Fig. 5. As found in the eight transformulas (corona bodies) of Fig. 5, the numbering of each vertex and the correspondence to each symmetry operation ($g \in \mathbf{D}_{2d}$) in the corona body are adopted in accord with the reference numbering shown in **1**. On the other hand, each vertex of the base body is numbered in accord with the inverse numbering shown in $\widetilde{\mathbf{1}}$.

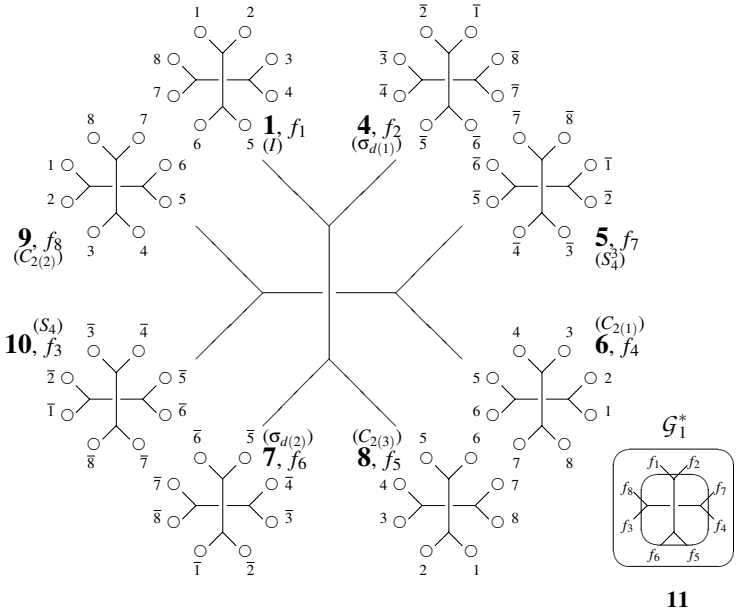

Figure 5: Mandala (a nested regular body) containing eight transformulas (f_1–f_8) at its vertices. The alignment shown in this diagram corresponds to the inverse numbering (**1**): $\mathcal{G}_1^* = \{f_1, f_2, f_7, f_4, f_5, f_6, f_3, f_8\}$. The full expression of the mandala is simplified into **11**. The number of fixed points is equal to $|\mathbf{D}_{2d}| = 8$ with respect to the one-membered orbit $\mathcal{G} = \{\mathcal{G}_1^*\}$.

Suppose that the eight positions of the reference (**1**) accommodate hydrogens to generate a H^8-transformula (**12** as f_1). On the action of $\mathbf{D}_{2d}$, the resulting set of transformulas, i.e., $\mathcal{G}_1^* = \{f_1, f_2, f_7, f_4, f_5, f_6, f_3, f_8\}$, is considered to construct a one-membered orbit $\mathcal{G}^* = \{\mathcal{G}_1^*\}$, as encircled in the simplified mandala (**11**). The one-membered orbit is governed by the LCR $\mathbf{D}_{2d}(/\mathbf{D}_{2d})$ and represents the symmetrical behavior of the H^8-transformula. Hence, the simplified mandala (**11**) is regarded as representing a molecule of $\mathbf{D}_{2d}$-symmetry.

The one-membered orbit ($\mathcal{G}^*$) governed by the LCR $\mathbf{D}_{2d}(/\mathbf{D}_{2d})$ is fixed by all of $p_g^{[R]}$ contained in the RRR $(\mathbf{C}_1\backslash)\mathbf{D}_{2d}$ ($g \in \mathbf{D}_{2d}$). Hence, the number of fixed points (assemblies) is calculated to be $|\mathbf{D}_{2d}|$ $(= 8)$. The term $8H^8$ is used to apply this result to chemical combinatorics,

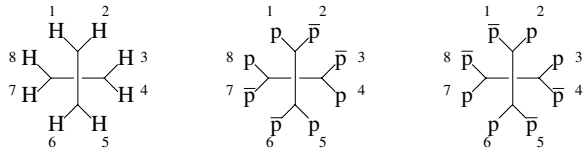

Figure 6: $\mathbf{D}_{2d}$-Molecules with H^8 (**12**) and $p^4\overline{p}^4$ (**13** and **14**). The symbols p and $\overline{p}$ represent a pair of enantiomeric proligands.

as discussed later.

Another $\mathbf{D}_{2d}$-molecule with $p^4\overline{p}^4$ (**13** as f_1) is also permissible because the $(\mathbf{C}_1\backslash)\mathbf{D}_{2d}$-orbit of the eight positions is enantiospheric. On the same line as above, the resulting set of transformulas, i.e., $\mathcal{G}_1^* = \{f_1, f_2, f_7, f_4, f_5, f_6, f_3, f_8\}$, is also considered to construct a one-membered orbit $\mathcal{G}^* = \{\mathcal{G}_1^*\}$ (**11**). The one-membered orbit ($\mathcal{G}^*$) in the simplified mandala (**11**) is governed by the LCR $\mathbf{D}_{2d}(/\mathbf{D}_{2d})$ and represents a molecule of $\mathbf{D}_{2d}$-symmetry. The number of fixed points (assemblies) is calculated to be $|\mathbf{D}_{2d}|$ $(= 8)$, because the orbit $\mathcal{G}^*$ is fixed once by every $p_g^{[R]}$ contained in the RRR $(\mathbf{C}_1\backslash)\mathbf{D}_{2d}$ ($g \in \mathbf{D}_{2d}$). To apply this result to chemical combinatorics, we use the term $8p^4\overline{p}^4$.

There exists a further $\mathbf{D}_{2d}$-molecule with $p^4\overline{p}^4$ (**14** as f_1), which is diastereomeric to **13**. The number of fixed points (assemblies) is also calculated to be $|\mathbf{D}_{2d}|$ $(= 8)$ on the same line. The molecules **13** and **14** are regarded as an extended case of so-called pseudoasymmetry, which is recognized in terms of *enantiosphericity* in the USCI approach [4].

With Segmentation Suppose that the segmentation pattern (**2**) shown in Fig. 3 is superposed onto each regular body (corona body) of the original mandala shown in Fig. 4. Thereby, we are able to obtain a mandala with segmented regular bodies, as shown in Fig. 7, where the segmentation causes the division of the eight positions in each regular body into four $\mathbf{C}_s$-segments, i.e., $\mathcal{A}_1$, $\mathcal{A}_2$, $\mathcal{A}_3$, and $\mathcal{A}_4$. They correspond to the right cosets shown in eq. 3 so that they construct a four-membered orbit, i.e., $\mathcal{A} = \{\mathcal{A}_1, \mathcal{A}_2, \mathcal{A}_3, \mathcal{A}_4\}$, which is governed by the RCR $(\mathbf{C}_s\backslash)\mathbf{D}_{2d}$.

The $\mathbf{C}_s$-segmentation, however, maintains the symmetrical feature of the simplified mandala (**22**). Thus, the one-membered orbit $\mathcal{G}^* = \{\mathcal{G}_1^*\}$ remains without division so as to be governed by the LCR $\mathbf{D}_{2d}(/\mathbf{D}_{2d})$. Because the one-membered orbit ($\mathcal{G}^*$) is fixed under $\mathbf{D}_{2d}$, the number of fixed points (assemblies) is calculated to be $|\mathbf{D}_{2d}|$ $(= 8)$.

The segmented mandala shown in Fig. 7 has a more chemical meaning by replacing each of the segment ($\mathcal{A}_1$, $\mathcal{A}_2$, $\mathcal{A}_3$, and $\mathcal{A}_4$) by a hydrogen atom. This procedure generates a reduced mandala with an allene molecule (H^4) as shown in Fig. 8, which has been discussed in Part 3 of this series [3]. The reduction also maintains the symmetrical feature of the simplified mandala (**31**) so that the one-membered orbit $\mathcal{G}^* = \{\mathcal{G}_1^*\}$ remains without division so as to be governed by the LCR $\mathbf{D}_{2d}(/\mathbf{D}_{2d})$. Because the one-membered orbit ($\mathcal{G}^*$) is fixed on the action of the eight operations of $\mathbf{D}_{2d}$, the number of fixed points (assemblies) is calculated to be $|\mathbf{D}_{2d}|$ $(= 8)$. The term $8H^4$ is used to apply this result to chemical combinatorics, where the coefficient 8 designates the number of fixed points (assemblies).

It is worthwhile to compare the methodology described in Part 3 [3] with the present one. By following the methodology of the USCI approach described in Part 3 [3], the one-membered

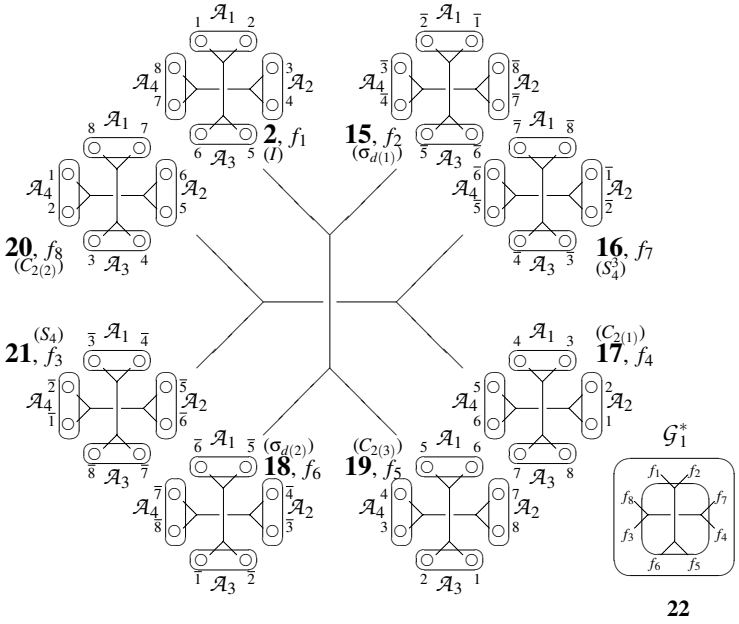

Figure 7: Mandala containing eight transformulas with segmentation (f_1–f_8). The alignment shown in this diagram corresponds to the inverse numbering (**1**): $\mathcal{G}_1^* = \{f_1, f_2, f_7, f_4, f_5, f_6, f_3, f_8\}$ in a clockwise direction. The full expression of the mandala is simplified into **22**. The number of fixed points is equal to $|\mathbf{D}_{2d}| = 8$ with respect to the one-membered orbit $\mathcal{G} = \{\mathcal{G}_1^*\}$.

orbit $\mathcal{G}^*$ in the mandala (e.g., **11**, **22**, and **31**) is characterized by a fixed-point vector (FPV), which is itemized with respect to the subgroups of $\mathbf{D}_{2d}$. Thus, the one-membered orbit $\mathcal{G}^*$ is characterized by an FPV = $(1,1,1,1,1,1,1,1)$ so that it is concluded to be governed by the RRR $(\mathbf{D}_{2d}\backslash)\mathbf{D}_{2d}$. This methodology enables us to itemize enumeration results with respect to the subgroups, i.e., the point-group symmetries of enumerated stereoisomers. On the other hand, the present methodology aims at obtaining the gross number of stereoisomers, where such symmetry itemization is not taken into consideration. Hence, the number of fixed points is evaluated by operating all of the symmetry operations of $\mathbf{D}_{2d}$ so as to be equal to the order of the group $\mathbf{D}_{2d}$, i.e., $|\mathbf{D}_{2d}| = 8$.

3.2 Assembled Mandalas

Assembled mandalas are further classified into two subcategories, i.e., mandalas with achiral **K**-assemblage for representing achiral stereoisomers and mandalas with chiral **K**-assemblage for representing pairs of enantiomers. In this subsection, the number of fixed points (assemblies) on the action of **G** is shown to be equal to $|\mathbf{G}|$ regardless of the chirality/achirality of **K**.

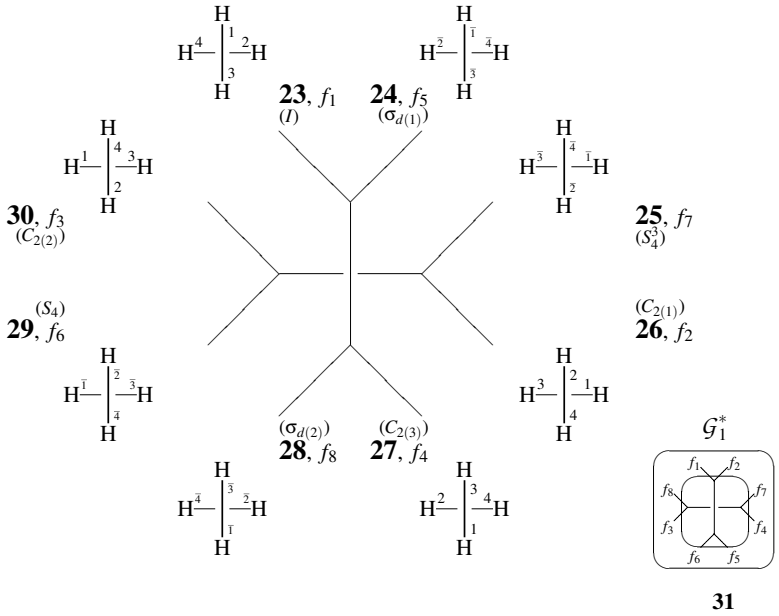

Figure 8: Reduced mandala for allene. The full expression of the mandala is simplified into **31**.

3.2.1 Achiral Assemblage

Without Segmentation Let us first examine a $\mathbf{C}_s$-assembled mandala (**40**) shown in Fig. 9. The eight transformulas (f_1–f_8) at its vertices are assembled into four assemblies, i.e., $\mathcal{A}_1^* = \{f_1, f_2\}$ = {**32**, **33**}, $\mathcal{A}_2^* = \{f_7, f_4\}$ = {**34**, **35**}, $\mathcal{A}_3^* = \{f_5, f_6\}$ = {**36**, **37**}, and $\mathcal{A}_4^* = \{f_3, f_8\}$ = {**38**, **39**}. According to this assemblage, the subduction (**3**) shown in Fig. 4 occurs so that the eight positions of each regular body are partitioned into four sets, i.e., $\{1,2\}$, $\{3,8\}$, $\{4,7\}$, and $\{5,6\}$ (cf. eq. 22). To show this partition explicitly, solid circles are depicted for the set of positions $\{1,2\}$ in Fig. 9. Thereby, the effect of the subduction remains, even if the $\mathbf{C}_s$-subduction pattern (the four oval boxes) is deleted.

On the action of $\mathbf{D}_{2d}$, the mandala **40** having the four-membered orbit of $\mathbf{C}_s$-assemblies ($\mathcal{A}^*$ = $\{\mathcal{A}_1^*, \mathcal{A}_2^*, \mathcal{A}_3^*, \mathcal{A}_4^*\}$) moves in accord with permutations due to the LCR $\mathbf{D}_{2d}(/\mathbf{C}_s)$. Even if all of the operations of $\mathbf{D}_{2d}$ are applied to the assembled mandala (**40**), the $\mathbf{C}_s$-assembly $\mathcal{A}_1^*$ (or $\mathcal{A}_3^*$) is fixed only under the action of the $\mathbf{C}_s$-subgroup so that $\mathcal{A}_1^*$ is fixed by I and $\sigma_{d(1)}$, giving $|\mathbf{C}_s|$ $(= 2)$ as the number of fixed points (assemblies). On the other hand, the $\mathbf{C}_s$-assembly $\mathcal{A}_2^*$ (or $\mathcal{A}_4^*$) is fixed only under the action of the $\mathbf{C}_s'$-subgroup so that $\mathcal{A}_1^*$ is fixed by I and $\sigma_{d(2)}$ ($\in \mathbf{C}_s'$), giving $|\mathbf{C}_s|$ $(= 2)$ as the number of fixed points (assemblies). Note that the $\mathbf{C}_s'$ is conjugate to $\mathbf{C}_s$ under the group $\mathbf{D}_{2d}$. Because the orbit $\mathcal{A}^*$ contains four ($= |\mathbf{D}_{2d}|/|\mathbf{C}_s| = 8/2 = 4$) assemblies, the total number of fixed points (assemblies) is calculated as follows

$$|\mathbf{C}_s| \times \frac{|\mathbf{D}_{2d}|}{|\mathbf{C}_s|} = |\mathbf{D}_{2d}| = 8. \tag{24}$$

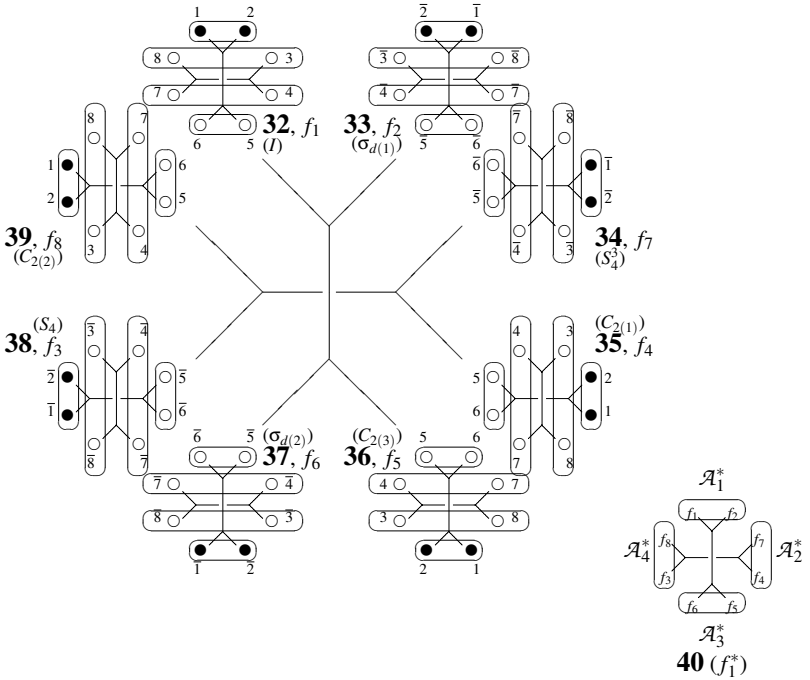

Figure 9: Mandala after $\mathbf{C}_s$-assemblage. The eight transformulas (f_1–f_8) at its vertices are assembled into four assemblies, i.e., $\mathcal{A}_1^* = \{f_1, f_2\}$, $\mathcal{A}_2^* = \{f_7, f_4\}$, $\mathcal{A}_3^* = \{f_5, f_6\}$, and $\mathcal{A}_4^* = \{f_3, f_8\}$. Solid circles are added to show the $\mathbf{C}_s$-symmetry explicitly. The full expression of the mandala is simplified into **40**.

Suppose that the eight positions of the reference (**1**) shown in Fig. 9 accommodate achiral proligands (H and X) and a pair of enantiomeric proligands (p and $\overline{\mathrm{p}}$) in accord with the division of the positions due to the subduction (eq. 22). Because the four $(\mathbf{C}_1\backslash)\mathbf{C}_s$-orbits are all enantiospheric, the corresponding sphericity index c_2 permits H^2, X^2, or $\mathrm{p}\overline{\mathrm{p}}$ for each of the $(\mathbf{C}_1\backslash)\mathbf{C}_s$-orbits. Thereby, the corresponding USCI-CF (unit subduced cycle index with chirality fittingness) c_2^4 allows us to generate several $\mathbf{C}_s$-molecule, as shown in Fig. 10.

Anyone of the $\mathbf{C}_s$-molecules can be used in place of the reference (**1**) shown in Fig. 9 so that the same simplified mandala (**40**) can be adopted to evaluate the corresponding number of fixed points (assemblies). It follows that the number of fixed points (assemblies) is calculated by eq. 24 for anyone of the $\mathbf{C}_s$-molecules collected in Fig. 10. The term $8\mathrm{H}^6\mathrm{X}^2$ (for **41**) etc. are used to apply this result to chemical combinatorics, where the coefficient 8 designates the number of fixed points.

It should be added here that **45** and **46** in Fig. 10 exhibit a kind of pseudoasymmetry, because the replacement of p/$\overline{\mathrm{p}}$ by X/Y generates a pair of enantiomers of the molecular formula $\mathrm{H}^6\mathrm{XY}$. On the same line. **47** and **48** also exhibit a kind of pseudoasymmetry.

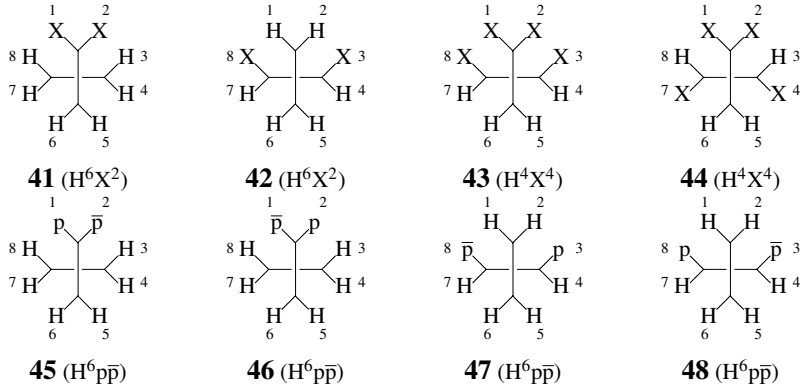

Figure 10: $\mathbf{C}_s$-Molecules with various molecular formulas. The symbols H and X represent achiral proligands and the symbols p and $\overline{\text{p}}$ represent a pair of enantiomeric proligands.

With Segmentation The $\mathbf{C}_s$-assembled mandala shown in Fig. 9 is further modified by $\mathbf{C}_s$-segmentation, as shown in Fig. 11. Thus, the $\mathbf{C}_s$-segmentation pattern (**2**) shown in Fig. 3 is superposed onto each subduced regular body shown in Fig. 9. Thereby, we obtain a $\mathbf{C}_s$-assembled mandala (**57**) with $\mathbf{C}_s$-segmentation, where the $\mathbf{C}_s$-assemblage is spontaneously accompanied with the subduction into $\mathbf{C}_s$, as shown in Fig. 11.

The same simplified mandala (**57**) can be generated alternatively, where the $\mathbf{C}_s$-subduction pattern (**3**) shown in Fig. 4 is superposed onto each $\mathbf{C}_s$-segmented regular body shown in Fig. 7. In spite of the different orders of superposition, the resulting mandala **57** is symmetrically equivalent to the mandala **40** under $\mathbf{D}_{2d}$.

By comparing between Fig. 9 and Fig. 11, we find that the $\mathbf{C}_s$-segmentation does not influence the apparent symmetrical feature of mandalas in the simplified level (i.e., **40** vs. **57**). Hence, we obtain the following $\mathbf{C}_s$-assemblies: $\mathcal{A}_1^* = \{f_1, f_2\} = \{\mathbf{49}, \mathbf{50}\}$, $\mathcal{A}_2^* = \{f_7, f_4\} = \{\mathbf{51}, \mathbf{52}\}$, $\mathcal{A}_3^* = \{f_5, f_6\} = \{\mathbf{53}, \mathbf{54}\}$, and $\mathcal{A}_4^* = \{f_3, f_8\} = \{\mathbf{55}, \mathbf{56}\}$. The orbit of $\mathbf{C}_s$-assemblies in **40**, i.e., $\mathcal{A}^* = \{\mathcal{A}_1^*, \mathcal{A}_2^*, \mathcal{A}_3^*, \mathcal{A}_4^*\}$, remains undisturbed to give the orbit of $\mathbf{C}_s$-assemblies in **57**. This means that the total number of fixed points is calculated by means of eq. 24.

On the other hand, the $\mathbf{C}_s$-assemblage (in **57**) influences intramolecular stereochemistry to cause the division of the orbit of segments $\mathcal{A} = \{\mathcal{A}_1, \mathcal{A}_2, \mathcal{A}_3, \mathcal{A}_4\}$ in each transformula (e.g., **49**). The division in the transformula **49** is diagrammatically interpreted as follows: the segment $\mathcal{A}_1$ (or $\mathcal{A}_3$) is isolated by the action of the subduction pattern (**3**) so as to generate a one-membered orbit, while the two segments $\mathcal{A}_2$ and $\mathcal{A}_4$ are regarded as remaining equivalent because the subduction pattern (**3**) ties the two segments. As a result, there emerge one-membered orbit $\{\mathcal{A}_1\}$, two-membered orbit $\{\mathcal{A}_2, \mathcal{A}_4\}$, and one-membered orbit $\{\mathcal{A}_4\}$, as found in each transformula (e.g., **49**). Obviously, each of the one-membered orbits ($\{\mathcal{A}_1\}$ and $\{\mathcal{A}_3\}$) is homospheric in terms of the criterion discussed in Part 1 so as to be characterized by the sphericity index a_1. The two-membered orbit $\{\mathcal{A}_2, \mathcal{A}_4\}$ is enantiospheric and characterized by the sphericity index c_2. The assignment of the sphericity indices is in accord with the subduction of the RCR:

$$(\mathbf{C}_s\backslash)\mathbf{D}_{2d} \downarrow \mathbf{C}_s = 2(\mathbf{C}_s\backslash)\mathbf{C}_s + (\mathbf{C}_1\backslash)\mathbf{C}_s, \tag{25}$$

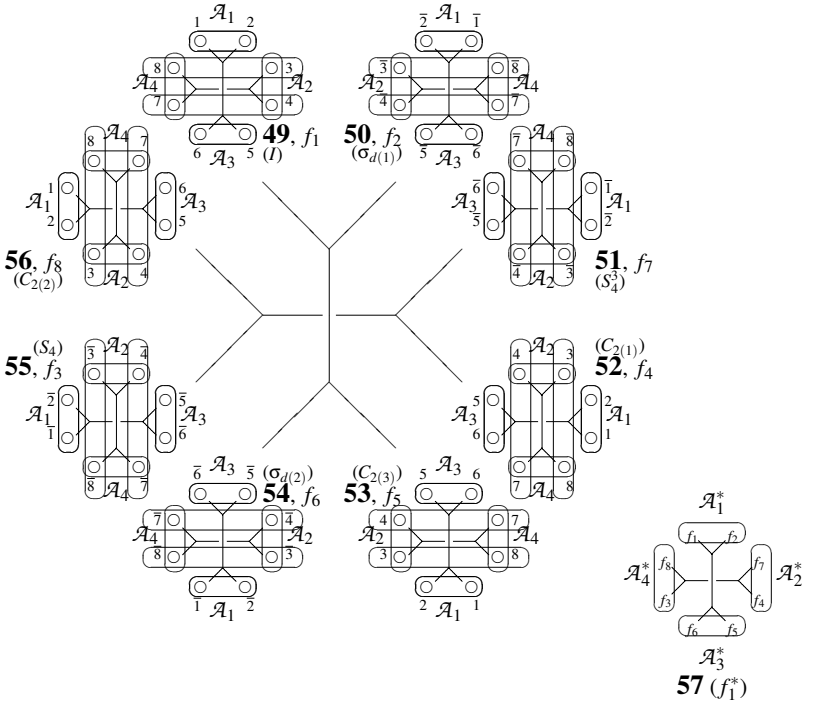

Figure 11: $\mathbf{C}_s$-Assembled mandala with $\mathbf{C}_s$-segmentation and $\mathbf{C}_s$-subduction. The full expression of the mandala is simplified into **57**.

where the sphericity index a_1 corresponding to the RCR $(\mathbf{C}_s\backslash)\mathbf{C}_s$ and the sphericity index c_2 corresponds to the RCR $(\mathbf{C}_1\backslash)\mathbf{C}_s$.

The sphericity index a_1 permits H or X for the one-membered orbit $\{\mathcal{A}_1\}$ (or $\{\mathcal{A}_4\}$), while the sphericity index c_2 permits H^2, X^2, or $p\overline{p}$ for the two-membered orbit $\{\mathcal{A}_2, \mathcal{A}_4\}$. Hence, several $\mathbf{C}_s$-molecules are generated, as shown in Fig. 12. Anyone of the $\mathbf{C}_s$-molecules shown Fig. 12 can be used in place of the reference (**49**) so that the same simplified mandala (**57**) can be adopted to evaluate the corresponding number of fixed points.

For example, Fig. 13 shows such a reduced mandala for characterizing the behavior of the mono-X-allene (**58**) of $\mathbf{C}_s$-symmetry. The symmetrical nature of the resulting simplified mandala (**69**) is common to that of the simplified mandala (**57**), where **69** is also assembled to generate four $\mathbf{C}_s$-assemblies: $\mathcal{A}_1^* = \{f_1, f_2\}$ = {**58**, **62**}, $\mathcal{A}_2^* = \{f_7, f_4\}$ = {**63**, **64**}, $\mathcal{A}_3^* = \{f_5, f_6\}$ = {**65**, **66**}, and $\mathcal{A}_4^* = \{f_3, f_8\}$ = {**67**, **68**}. This means that the number of fixed points (i.e., the number of fixed assemblies) is calculated by eq. 24 for **58**. On the same line, eq. 24 holds true for anyone of the $\mathbf{C}_s$-molecules collected in Fig. 12. It follows that the terms $8H^3X$ (for **58**), $8H^2p\overline{p}$ (for **59**) and $8HXp\overline{p}$ (for each of **60** and **61**) are used to apply these results to chemical combinatorics, where the coefficient 8 designates the number of fixed points (assemblies).

58 (H^3X)

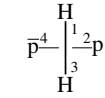

59 ($H^2p\overline{p}$)

60 ($HXp\overline{p}$)

61 ($HXp\overline{p}$)

Figure 12: $\mathbf{C}_s$-Molecules with various molecular formulas. The symbols H and X represent achiral proligands and the symbols p and $\overline{\text{p}}$ represent a pair of enantiomeric proligands.

To show that any segmentation does not influence the apparent symmetrical feature of mandalas in the simplified level, Fig. 14 shows a $\mathbf{C}_2'$-segmentation, where the corresponding $\mathbf{C}_2'$-segmentation pattern is superposed onto each transformula shown in Fig. 9. Thereby, we obtain the following $\mathbf{C}_s$-assemblies: $\mathcal{A}_1^* = \{f_1, f_2\}$ = {**70**, **71**}, $\mathcal{A}_2^* = \{f_7, f_4\}$ = {**72**, **73**}, $\mathcal{A}_3^* = \{f_5, f_6\}$ = {**74**, **75**}, and $\mathcal{A}_4^* = \{f_3, f_8\}$ = {**76**, **77**}. By comparing Fig. 14 with Fig. 9 (and Fig. 11), we find that the $\mathbf{C}_2'$-segmentation does not influence the apparent symmetrical feature of mandalas in the simplified level (cf. **40**, **57**, and **78**). In other words, the orbit of $\mathbf{C}_s$-assemblies in **78**, i.e., $\mathcal{A}^* = \{\mathcal{A}_1^*, \mathcal{A}_2^*, \mathcal{A}_3^*, \mathcal{A}_4^*\}$, remains undisturbed so that the total number of fixed points (assemblies) is calculated by means of eq. 24.

Chemically speaking, however, the $\mathbf{C}_2'$-segmentation shown in Fig. 14 does not give concrete molecules so long as the regular body (**1**) is selected. A chemically meaningful example of the $\mathbf{C}_2'$-segmentation has been once discussed by selecting adamantane-2,6-dione as another regular body of $\mathbf{D}_{2d}$ in Chapter 8 of Fujita's book [4], although the concept of mandala was not been involved. Eight hydrogen atoms in the four methylenes of adamantane-2,6-dione construct an orbit governed by the RRR $(\mathbf{C}_1\backslash)\mathbf{D}_{2d}$, where each of the four methylenes is regarded as a $\mathbf{C}_2'$-segment. The four-membered orbit of the four methylenes is governed by the RCR $(\mathbf{C}_2'\backslash)\mathbf{D}_{2d}$.

It is worthwhile again to compare the methodology described in Part 3 [3] with the present one. By following the methodology of the USCI approach described in Part 3 [3], the four-membered orbit $\mathcal{A}^*$ $(= \{\mathcal{A}_1^*, \mathcal{A}_2^*, \mathcal{A}_3^*, \mathcal{A}_4^*\})$ in the simplified mandala (e.g., **40**, **57**, **69**, or **78**) is characterized by an FPV = $(4,0,0,0,2,0,0,0,0)$, which corresponds to the LCR $\mathbf{D}_{2d}(/\mathbf{C}_s)$. The FPV allows us to classify enumerated stereoisomers into respective point-group symmetries. Because the present methodology aims at obtaining the gross number of stereoisomers, the number of fixed points (assemblies) is evaluated by operating all of the symmetry operations of $\mathbf{D}_{2d}$ so as to be equal to the order of the group $\mathbf{D}_{2d}$, i.e., $|\mathbf{D}_{2d}| = 8$.

3.2.2 Chiral Assemblage

Without Segmentation A mandala with chiral assemblage gives a different mode of fixation, in which a pair of enantiomers participates. For example, Fig. 15 shows that eight transformulas (f_1–f_8) at the vertices of a $\mathbf{C}_2'$-assembled mandala (**87**) are assembled into four assemblies, i.e., $\mathcal{B}_1^* = \{f_1, f_4\}$ = {**79**, **82**}, $\mathcal{B}_2^* = \{f_7, f_6\}$ = {**81**, **84**}, $\mathcal{B}_3^* = \{f_5, f_8\}$ = {**83**, **86**}, and $\mathcal{B}_4^* = \{f_2, f_3\}$

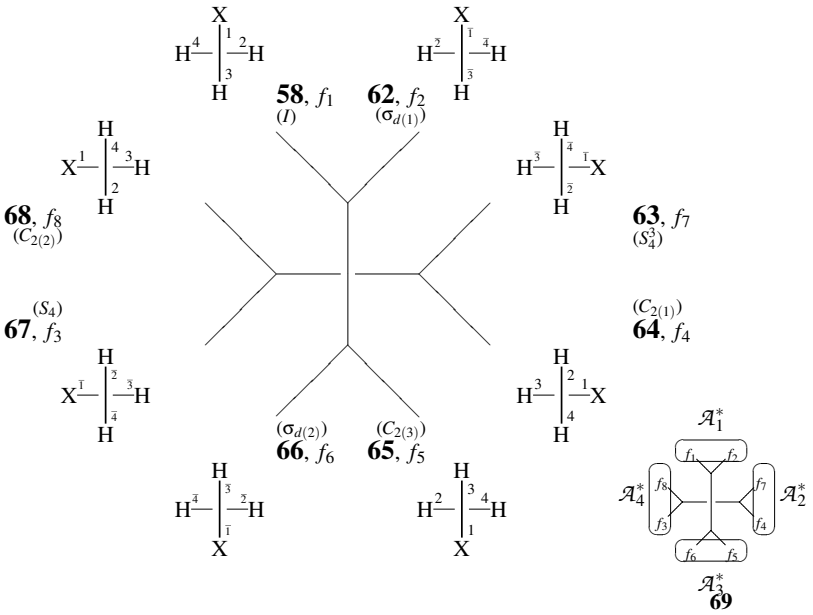

Figure 13: Reduced mandala for mono-X-allene of $\mathbf{C}_s$-symmetry. The full expression of the mandala is simplified into **69**.

= {**80**, **81**}. Although these four assemblies are equivalent on the action of $\mathbf{D}_{2d}$, they become non-equivalent under $\mathbf{D}_2$ so as to be divided into two sets, $\{\mathcal{B}_1^*, \mathcal{B}_3^*\}$ and $\{\mathcal{B}_2^*, \mathcal{B}_4^*\}$, which indicate the appearance of a pair of enantiomers (**79** and **80**). According to this assemblage, the subduction occurs spontaneously so that the eight positions of each regular body are partitioned into four sets, i.e., $\{2,3\}$, $\{1,4\}$, $\{5,8\}$, and $\{6,7\}$, as found in **79**. To show the effect of this partition explicitly, solid circles are placed on the set of positions $\{2,3\}$ in Fig. 15.

Even if all of the operations of $\mathbf{D}_{2d}$ are applied to the assembled mandala (**87**), the $\mathbf{C}_2'$-assembly $\mathcal{B}_1^*$ (or $\mathcal{B}_3^*$) is fixed only under the action of the $\mathbf{C}_2'$-subgroup. Thus, $\mathcal{B}_1^*$ is fixed by I and $C_{2(1)}$, giving $|\mathbf{C}_2'|$ $(=2)$ as the number of fixed points (assemblies). On the other hand, the $\mathbf{C}_2'$-assembly $\mathcal{B}_2^*$ (or $\mathcal{B}_4^*$) is fixed only under the action of the $\mathbf{C}_2''$-subgroup so that $\mathcal{B}_2^*$ is fixed by I and $C_{2(2)}$ $(\in \mathbf{C}_2'')$, giving $|\mathbf{C}_2|''$ $(=2)$ as the number of fixed points. Note that the $\mathbf{C}_2''$ is conjugate to $\mathbf{C}_2'$ under the group $\mathbf{D}_{2d}$. Because the orbit $\mathcal{B}^*$ contains four $(= |\mathbf{D}_{2d}|/|\mathbf{C}_2'| = 8/2 = 4)$ assemblies, the total number of fixed points (assemblies) is calculated as follows

$$|\mathbf{C}_2'| \times \frac{|\mathbf{D}_{2d}|}{|\mathbf{C}_2'|} = |\mathbf{D}_{2d}| = 8. \tag{26}$$

It should be noted that one half of the number of fixed points (assemblies) is concerned with a chiral stereoisomer represented by $\mathcal{B}_1^*$ (plus $\mathcal{B}_3^*$), while the other half is concerned with its enantiomer represented by $\mathcal{B}_2^*$ (plus $\mathcal{B}_4^*$).

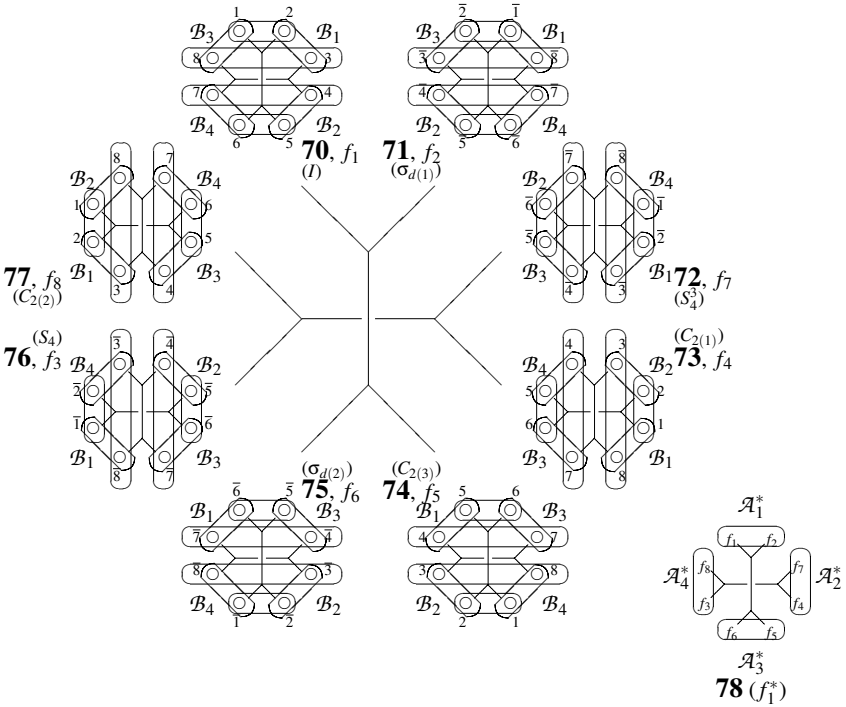

Figure 14: $\mathbf{C}_s$-Assembled mandala with $\mathbf{C}_2'$-segmentation and $\mathbf{C}_s$-subduction. The full expression of the mandala is simplified into **78**.

To generate $\mathbf{C}_2'$-molecules, a selected set of achiral proligands (H and X) and a pair of enantiomeric proligands (p and $\overline{\mathrm{p}}$) is placed on the eight positions in accord with the division of the positions due to the subduction (Fig. 15). Because the four $(\mathbf{C}_1\backslash)\mathbf{C}_2'$-orbits are all hemispheric, the corresponding sphericity index b_2 permits H^2, X^2, or p^2 (or $\overline{\mathrm{p}}^2$) for each of the $(\mathbf{C}_1\backslash)\mathbf{C}_s$-orbits. Thereby, the corresponding USCI-CF b_2^4 indicates that several $\mathbf{C}_2'$-molecule can be generated as shown in Fig. 16, where an arbitrary enantiomer is depicted for each enantiomeric pair.

Anyone of the $\mathbf{C}_2'$-molecules can be used in place of the reference (**79**) so as to give the same simplified mandala (**87**). Hence, the corresponding number of fixed points (assemblies) can be evaluated in terms of the simplified mandala (**87**). In other words, the number is calculated by eq. 26 for anyone of the $\mathbf{C}_2'$-molecules collected in Fig. 16. The term $8\mathrm{H}^6\mathrm{X}^2$ (for **88**), $8\times\frac{1}{2}(\mathrm{H}^6\mathrm{p}^2+\mathrm{H}^6\overline{\mathrm{p}}^2)$ (for **92**), and so on are used to apply this result to chemical combinatorics, where the coefficient 8 designates the number of fixed points. Note that one half of the number of fixed points for **92** is concerned with a chiral stereoisomer represented by $\mathrm{H}^6\mathrm{p}^2$ while the other half is concerned with its enantiomer represented by $\mathrm{H}^6\overline{\mathrm{p}}^2$. This means that fixed points (assemblies) should be counted by using the term $\frac{1}{2}(\mathrm{H}^6\mathrm{p}^2+\mathrm{H}^6\overline{\mathrm{p}}^2)$ as a unit. Strictly speaking,

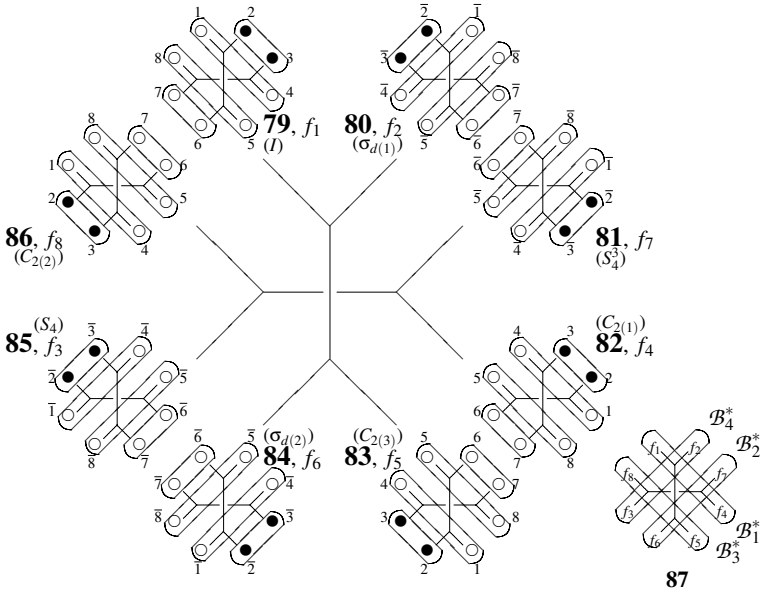

Figure 15: $\mathbf{C}_2'$-Assembled mandala. The eight transformulas (f_1–f_8) at its vertices are assembled into four assemblies, i.e., $\mathcal{B}_1^* = \{f_1, f_4\}$, $\mathcal{B}_2^* = \{f_6, f_7\}$, $\mathcal{B}_3^* = \{f_5, f_8\}$, and $\mathcal{B}_4^* = \{f_2, f_3\}$. Solid circles are added to show the $\mathbf{C}_2'$-symmetry explicitly. The full expression of the mandala is simplified into **87**.

even the term H^6X^2 for **88** and **89** should be regarded as $\frac{1}{2}(H^6X^2 + \overline{H^6X^2})$. Because of $\overline{H} = H$ and $\overline{X} = X$ for atoms (or achiral ligands), the term $\frac{1}{2}(H^6X^2 + \overline{H^6X^2})$ is equal to H^6X^2.

The molecules (**96**, **97**, **98**, and **99**) collected in the bottom row of Fig. 16 can be derived from Fig. 15 by an alternative mode of placement. They are depicted in connection with the corresponding diastereomeric molecules (**92**, **93**, **94**, and **95**) shown in the middle row.

With Segmentation Suppose that the $\mathbf{C}_s$-segmentation pattern (**2**) shown in Fig. 3 is superposed onto each subduced regular body shown in Fig. 16. Thereby, the $\mathbf{C}_2'$-assembled mandala (Fig. 16) is further modified by the $\mathbf{C}_s$-segmentation to give another $\mathbf{C}_2'$-assembled mandala (**108**) as shown in Fig. 17.

The same mandala (**108**) can be generated alternatively, where the $\mathbf{C}_s$-subduction pattern is superposed onto each $\mathbf{C}_s$-segmented regular body shown in Fig. 7. In spite of the different orders of superposition, the resulting mandala **108** is symmetrically equivalent to the mandala **87** under $\mathbf{D}_{2d}$.

The $\mathbf{C}_s$-segmentation does not influence the apparent symmetrical feature of mandalas in the simplified level (i.e., **87** vs. **108**). This means that the four $\mathbf{C}_2'$-assemblies remain undisturbed in **108**, i.e., $\mathcal{B}_1^* = \{f_1, f_4\}$ = {**100**, **103**}, $\mathcal{B}_2^* = \{f_7, f_6\}$ = {**102**, **105**}, $\mathcal{B}_3^* = \{f_5, f_8\}$ = {**104**, **107**}, and $\mathcal{B}_4^* = \{f_2, f_3\}$ = {**101**, **106**}, The total number of fixed points (assemblies) is calculated by

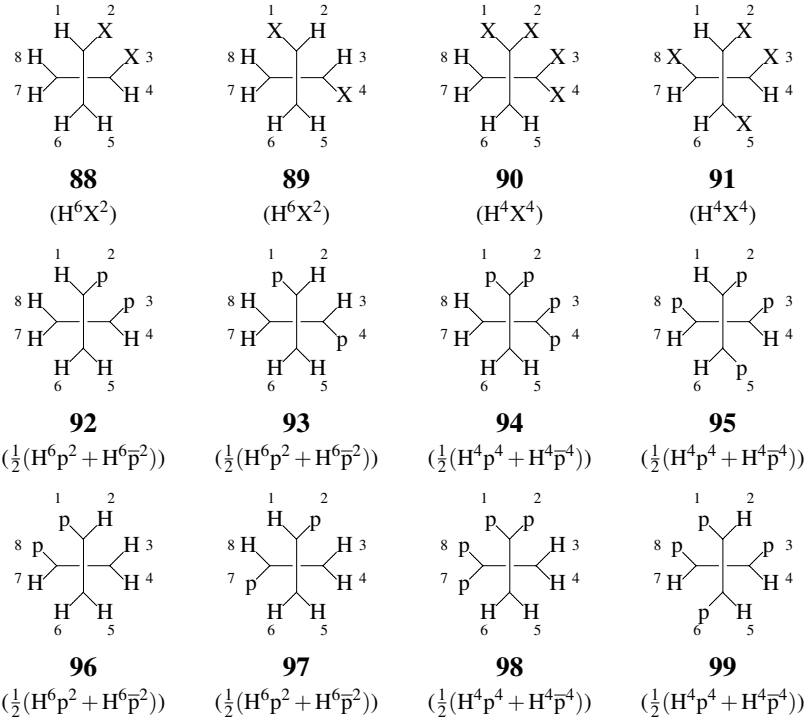

Figure 16: $\mathbf{C}_2'$-Molecules with various molecular formulas. The symbols H and X represent achiral proligands and the symbols p and $\overline{\text{p}}$ represent a pair of enantiomeric proligands.

means of eq. 26.

As a result of the $\mathbf{C}_2'$-assemblage (in **108**), the orbit of $\mathbf{C}_s$-segments $\mathcal{A} = \{\mathcal{A}_1, \mathcal{A}_2, \mathcal{A}_3, \mathcal{A}_4\}$ in each transformula (e.g., **100**) is divided into two two-membered orbits, i.e., $\{\mathcal{A}_1, \mathcal{A}_2\}$ and $\{\mathcal{A}_3, \mathcal{A}_4\}$. Note that the subduction pattern ties the two segments ($\mathcal{A}_1$ and $\mathcal{A}_2$) as well as the other two segments ($\mathcal{A}_3$ and $\mathcal{A}_4$). Each of the two-membered orbit is hemispheric and characterized by the sphericity index b_2.

The sphericity index b_2 permits H^2, X^2, p^2 ($\overline{p}^2$), or q^2 ($\overline{q}^2$) for each of the two-membered orbits ($\{\mathcal{A}_1, \mathcal{A}_2\}$ and $\{\mathcal{A}_3, \mathcal{A}_4\}$). It follows that several $\mathbf{C}_2'$-molecules are generated, as shown in Fig. 18. The molecules (**110** and **111**) collected in the bottom row of Fig. 18 can be derived from **100** by the initial placement of $\overline{\text{p}}$ (or $\overline{\text{q}}$) on $\mathcal{A}_1$ and $\mathcal{A}_2$. They are depicted in connection with the corresponding diastereomeric molecules (**112** and **113**) in the middle row.

Anyone of the $\mathbf{C}_2'$-molecules shown in Fig. 18 can be used in place of the reference (**100**) so that the same simplified mandala (**108**) can be used to evaluate the corresponding number of fixed points (assemblies). Hence, the number of fixed points (assemblies) is calculated by eq. 26 for anyone of the $\mathbf{C}_2'$-molecules collected in Fig. 18. The terms $8H^2X^2$ (for **109**), $8 \times \frac{1}{2}(H^2p^2 + H^2\overline{p}^2)$ (for **110** and **112**), $8 \times \frac{1}{2}(p^2q^2 + \overline{p}^2\overline{q}^2)$ (for **111** and **113**) are used to apply these

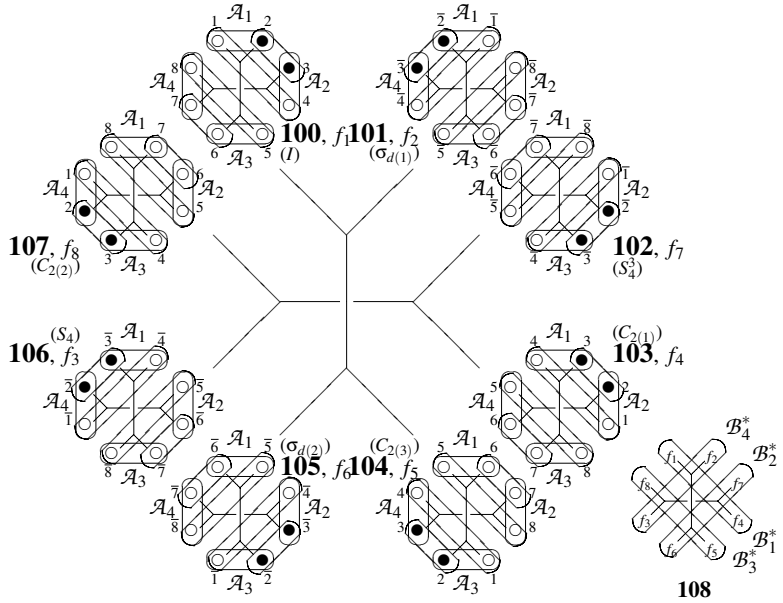

Figure 17: $\mathbf{C}_2'$-assembled mandala with $\mathbf{C}_s$-segmentation. The eight transformulas (f_1–f_8) at its vertices are assembled into four assemblies, i.e., $\mathcal{B}_1^* = \{f_1, f_4\}$, $\mathcal{B}_2^* = \{f_6, f_7\}$, $\mathcal{B}_3^* = \{f_5, f_8\}$, and $\mathcal{B}_4^* = \{f_2, f_3\}$. Solid circles are added to show the $\mathbf{C}_2'$-symmetry explicitly. The full expression of the mandala is simplified into **108**.

results to chemical combinatorics, where the coefficient 8 designates the number of fixed points (assemblies).

Although Fig. 17 aims at exhibiting the effect of segmentation, the diagrams in Fig. 17 are too complicated to understand the effect at a glance because they involve a subduction pattern along with a segmentation pattern. Note that the effect of subduction can be fully expressed by solid circles without such a subduction pattern. Hence, it is informative to compare Fig. 17 with Fig. 15 after the subduction pattern for $\mathbf{C}_2'$ is deleted.

By deleting the $\mathbf{C}_2'$-subduction pattern, the reference transformula **79** shown in Fig. 15 is converted into **114** as shown in Fig. 19, where the solid circles assure the $\mathbf{C}_2'$-symmetry of **114**. The resulting transformula **114** can be used as a reference in place of **79** so as to generate another mandala which is characterized also by the simplified mandala **87** (Fig. 15). Then, the solid circles of **114** are replaced by X and the open circles are replaced by H so as to generate the $\mathbf{C}_2'$-molecule (**88**) as one enantiomer.

On the other hand, the reference transformula **100** shown in Fig. 17 is converted into **115** shown in Fig. 19 by deleting the $\mathbf{C}_2'$-subduction pattern. Even with the $\mathbf{C}_s$-segmentation, the solid circles also assure the $\mathbf{C}_2'$-symmetry of **115**. The resulting transformula **115** can be used as a reference in place of **100** so as to generate another mandala which is characterized also by the simplified mandala **108** (Fig. 17). The four segments (i.e., $\mathcal{A}_1, \mathcal{A}_2, \mathcal{A}_3, \mathcal{A}_4$, cf. **100**), however,

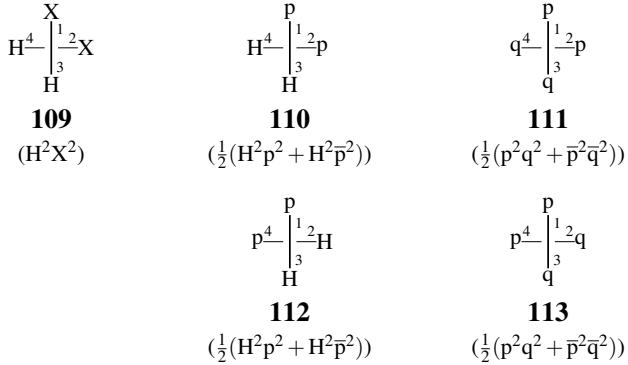

Figure 18: $\mathbf{C}_2'$-Molecules with various molecular formulas. The symbols H and X represent achiral proligands and the symbols p/$\overline{\text{p}}$ and q/$\overline{\text{q}}$ represent pairs of enantiomeric proligands.

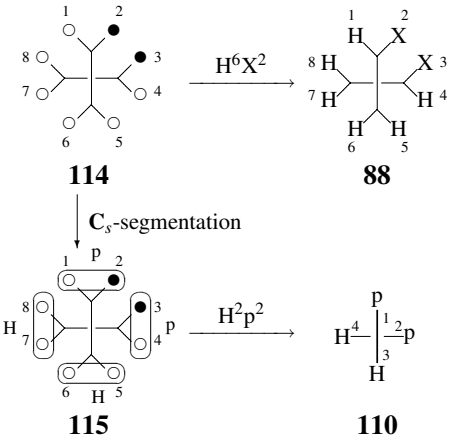

Figure 19: Relationship between $\mathbf{C}_2'$-molecules based on different skeletons.

are not equivalent so as to be divided into two categories, i.e., $\{\mathcal{A}_1, \mathcal{A}_2\}$ and $\{\mathcal{A}_3, \mathcal{A}_4\}$. Among them, the two segments ($\mathcal{A}_1$ and $\mathcal{A}_2$) containing a solid circle in **115** are replaced by p and the remaining two segments ($\mathcal{A}_3$ and $\mathcal{A}_4$) are replaced by H. Thereby, we obtain the $\mathbf{C}_2'$-molecule (**110**) as one enantiomer.

As shown in Fig. 19, **115** is alternatively obtained by the direct $\mathbf{C}_s$-segmentation of **114**. Literally speaking, the process of converting **114** into **115** cannot be realized by chemical reactions so that this segmentation process tends to be regarded as having a mathematical or symmetrical meaning only. However, there are many examples in which segmentation processes have chemical meanings. For example, suppose that the proligands p in **110** are replaced by chiral ligands

R-CXYZ and the scheme shown in Fig. 19 is redrawn in accord with this replacement. Then, an example of more chemical meaning can be obtained (this problem is left as an exercise for readers). Even if the scheme is regarded as mathematical, it is reasonable to say that the scheme shown in Fig. 19 provides a succinct model in which organic chemists regard a set of atoms (i.e., a segment in the present terminology) as a ligand.

3.3 Characterization of Mandalas

As discussed in detail in the preceding subsections (Subsections 3.2.1 and 3.2.2), a stereoisomer of **K**-symmetry corresponds to a **K**-assembled mandala, in which each of the $|\mathbf{G}|/|\mathbf{K}|$ assemblies is fixed on the action of the operators of **K** or its conjugate subgroups. Because the number of fixed points (assemblies) is equal to $|\mathbf{K}|$ for each of the $|\mathbf{G}|/|\mathbf{K}|$ assemblies, the total number of fixed points (assemblies) for the **K**-assembled mandala (and the stereoisomer of **K**-symmetry) is calculated to be

$$|\mathbf{K}| \times \frac{|\mathbf{G}|}{|\mathbf{K}|} = |\mathbf{G}|. \tag{27}$$

This equation is a general expression of eq. 24 (for $\mathbf{K} = \mathbf{C}_s$) and eq. 26 (for $\mathbf{K} = \mathbf{C}_2'$) for $\mathbf{G} = \mathbf{D}_{2d}$. The results described for mandalas without assemblage (e.g., Figs. 5, 7, 8) represent a special case in which **K** is equal to $\mathbf{D}_{2d}$ for $\mathbf{G} = \mathbf{D}_{2d}$.

Equation 27 holds true for any subgroup **K**, whether the **K** is achiral (cf. Subsection 3.2.1) or chiral (cf. Subsection 3.2.2). This is summarized for further discussions as a theorem:

Theorem 1 (Number of Fixed Assemblies) Suppose that a given skeleton of **G**-symmetry has $|\mathbf{G}|/|\mathbf{H}|$ of **H**-segments which construct an orbit governed by the RCR $(\mathbf{H}\backslash)\mathbf{G}$ and that the **H**-segments accommodate achiral or chiral proligands to give a stereoisomer of **K**-symmetry. Then, the corresponding **K**-assembled mandala is generated so as to exhibit the following features:

1. The action of all the operations of **G** on the $|\mathbf{G}|/|\mathbf{K}|$ assemblies of the **K**-assembled mandala gives the number of fixed points (the number of fixed assemblies) to be equal to $|\mathbf{G}|$.

2. The **H**-segmentation does not disturb the number of fixed points (assemblies) calculated above.

□

It should be noted that the group **K** and **H** may be any subgroups of **G**. This means that Theorem 1 holds true for any molecular formula and any symmetry of the stereoisomer at issue. Moreover, the $|\mathbf{G}|/|\mathbf{H}|$-membered set of **H**-segments can multiply participates in the process of derivation of the stereoisomer (Theorem 1) where **H** runs over the non-redundant set of subgroups of **G**. When the multiplicity is represented by $\alpha_{\mathbf{H}}$, we can say generally that the skeleton of Theorem 1 has orbits of segments governed by the sum of such RCRs as:

$$\sum_{\mathbf{H}} \alpha_{\mathbf{H}} (\mathbf{H}\backslash)\mathbf{G}, \tag{28}$$

where the summation is concerned with **H**, which moves over the non-redundant set of subgroups of **G**. Thus, the second proposition of Theorem 1 can be more generally regarded as being based on eq. 28 in place of the simple **H**-segmentation.

It should be added here that the first proposition of Theorem 1 describes the context which is essentially equivalent to the proof of the Cauthy-Frobenius Lemma (so-called Burnside's Lemma, cf. Theorem 5.2 in Chapter 5 of Ref. [22] and Theorem 13.1 in Chapter 13 of Fujita's book [4]). A new matter of the present theorem is the discussions on the chirality/achirality of (pro)ligands by using the concept of mandalas.

4 Combinatorial Enumeration

4.1 The Number of Fixed Assemblies per Stereoisomer

To generalize the discussions described in Section 3, suppose that a **G**-skeleton having r substitution positions accommodates r of achiral or chiral proligands, which are selected from the following set:

$$\mathbf{X} = \{\mathrm{X}_1, \mathrm{X}_2, \ldots, \mathrm{X}_t; \mathrm{p}_1, \mathrm{p}_2, \ldots, \mathrm{p}_u; \overline{\mathrm{p}}_1, \overline{\mathrm{p}}_2, \ldots, \overline{\mathrm{p}}_u\}, \tag{29}$$

where the symbols t and u represent non-negative integers ($tu \neq 0$); each X_i is achiral; and a pair of p_i and $\overline{\mathrm{p}}_i$ represents an enantiomeric pair. Note that the term *proligands* is used to designate a hypothetical ligand which is structureless but has chirality/achirality in accord with Fujita's proligand method [15, 16, 17] and with Fujita's USCI approach [4]. For the sake of convenience, we will use the term "ligands" in place of the term "proligands" so long as this usage would cause no confusion.

Suppose that a stereoisomer of **K**-symmetry is generated by the substitution of θ_1 of X_1, θ_2 of X_2, …, θ_t of X_t; θ'_1 of p_1, θ'_2 of p_2, …, θ'_u of p_u; and θ''_1 of $\overline{\mathrm{p}}_1$, θ''_2 of $\overline{\mathrm{p}}_2$, …, θ''_u of $\overline{\mathrm{p}}_u$, where the symbols, θ_i, θ'_i, and θ''_i, represent non-negative integers which satisfy the following partition:

$$\begin{aligned}[\theta]: \quad & \theta_1 + \theta_2 + \cdots + \theta_t + \\ & \theta'_1 + \theta'_2 + \cdots + \theta'_u + \\ & \theta''_1 + \theta''_2 + \cdots + \theta''_u = r. \end{aligned} \tag{30}$$

Whether **K** is achiral or chiral, the molecular formula W_θ is represented by the following equation:

$$W_\theta = \mathrm{X}_1^{\theta_1}\mathrm{X}_2^{\theta_2}\cdots\mathrm{X}_t^{\theta_t}\mathrm{p}_1^{\theta'_1}\mathrm{p}_2^{\theta'_2}\cdots\mathrm{p}_u^{\theta'_u}\overline{\mathrm{p}}_1^{\theta''_1}\overline{\mathrm{p}}_2^{\theta''_2}\cdots\overline{\mathrm{p}}_u^{\theta''_u} \tag{31}$$

It should be noted that a chiral stereoisomer of **K**-symmetry corresponds to a mandala having $|\mathbf{G}|/2|\mathbf{K}|$ assemblies of one chirality and $|\mathbf{G}|/2|\mathbf{K}|$ assemblies of the opposite chirality, as shown in Subsection 3.2.2. Hence, a pair of such enantiomeric stereoisomers must be taken into consideration so as to have the following molecular formula:

$$\begin{aligned} W_\theta \;=\; & \frac{1}{2}\Big\{\mathrm{X}_1^{\theta_1}\mathrm{X}_2^{\theta_2}\cdots\mathrm{X}_t^{\theta_t}\mathrm{p}_1^{\theta'_1}\mathrm{p}_2^{\theta'_2}\cdots\mathrm{p}_u^{\theta'_u}\overline{\mathrm{p}}_1^{\theta''_1}\overline{\mathrm{p}}_2^{\theta''_2}\cdots\overline{\mathrm{p}}_u^{\theta''_u} + \\ & \mathrm{X}_1^{\theta_1}\mathrm{X}_2^{\theta_2}\cdots\mathrm{X}_t^{\theta_t}\mathrm{p}_1^{\theta''_1}\mathrm{p}_2^{\theta''_2}\cdots\mathrm{p}_u^{\theta''_u}\overline{\mathrm{p}}_1^{\theta'_1}\overline{\mathrm{p}}_2^{\theta'_2}\cdots\overline{\mathrm{p}}_u^{\theta'_u}\Big\}. \end{aligned} \tag{32}$$

If we use eq. 32 as a molecular formula W_θ in place of eq. 31, two modes of partitions among $[\theta]$ (eq. 30), i.e., $[\theta'_1\cdots$ (for p), $\theta''_1\cdots$ (for $\overline{\mathrm{p}}$)] and $[\theta''_1\cdots$ (for p), $\theta'_1\cdots$ (for $\overline{\mathrm{p}}$)], gives the same molecular formula. This duplication should be omitted by modifying the partition $[\theta]$ (eq. 30).

Obviously, we can derive a molecular formula for an achiral stereoisomer by placing $\theta'_i = \theta''_i$ ($i = 1, 2, \ldots, u$) in eq. 31 or eq. 32, i.e.,

$$W_\theta = X_1^{\theta_1} X_2^{\theta_2} \cdots X_t^{\theta_t} p_1^{\theta'_1} p_2^{\theta'_2} \cdots p_u^{\theta'_u} \overline{p}_1^{\theta'_1} \overline{p}_2^{\theta'_2} \cdots \overline{p}_u^{\theta'_u}. \tag{33}$$

Theorem 1 indicates that the stereoisomer of the molecular formula W_θ (eq. 31) is characterized by $|\mathbf{G}|$ (the number of fixed points), even when its symmetry $\mathbf{K}$ is anyone of the subgroups of $\mathbf{G}$.

The $\mathbf{K}$-symmetry described in Theorem 1 moves over the subgroups of $\mathbf{G}$ so as to result in the occurrence of one or more stereoisomers of various subsymmetries of $\mathbf{G}$, even though a given partition $[\theta]$ is tentatively fixed. Let the symbol B_θ denote the number of such stereoisomers as assigned to the partition $[\theta]$ (eq. 30). Then, the generating function for B_θ is expressed as follows:

$$\sum_{[\theta]} B_\theta W_\theta \tag{34}$$

where the summation is concerned with all of the partitions ($[\theta]$) shown in eq. 30 and the molecular formula is represented by W_θ (eq. 31). Because each stereoisomer (or each pair of enantiomers) appearing in eq. 34 has $|\mathbf{G}|$ fixed points as summarized in Theorem 1, the numbers of fixed points (assemblies) appear as the coefficients of the terms in the following generating function:

$$|\mathbf{G}| \sum_{[\theta]} B_\theta W_\theta. \tag{35}$$

4.2 Number of Fixed Assemblies per Permutation

4.2.1 Sphericities of Cycles

When $|\mathbf{G}|/|\mathbf{H}|$ of $\mathbf{H}$-segments in the skeleton of $\mathbf{G}$-symmetry (Theorem 1) accommodate achiral or chiral proligands according to the partition shown in eq. 30, two alternative viewpoints for evaluating fixed points (assemblies) emerge:

1. The resulting stereoisomer is characterized by the molecular formula W_θ (eq. 31) and the symmetry $\mathbf{K}$. Each $\mathbf{K}$-stereoisomer (i.e., each $\mathbf{K}$-assembled mandala) is moved by all of the operations of $\mathbf{G}$ so as to give $|\mathbf{G}|$ as the number of fixed points (assemblies), regardless of the $\mathbf{K}$. This procedure has provided us with a method for evaluating the number of fixed points (assemblies) *per stereoisomer*, as described in the preceding subsections (Subsections 3.2.1, 3.2.2, and 4.1). When the partition $[\theta]$ of W_θ runs to cover all stereoisomers, the total numbers of fixed points (assemblies) are obtained (cf. eq. 35).

2. On the other hand, the permutation $p_g^{[R]}$ corresponding to each $g(\in \mathbf{G})$ fixes zero or more $\mathbf{K}$-assemblies of every $\mathbf{K}$-assembled mandala, where the $\mathbf{K}$ runs over the subgroups of $\mathbf{G}$. This procedure gives a basis to a method for evaluating the number of fixed points (assemblies) *per permutation*. When g runs over $\mathbf{G}$, the total numbers of fixed points (assemblies) are obtained alternatively.

In this subsection, the latter viewpoint shall be examined in detail. Let a permutation $p_g^{[R]}$ (for $g \in \mathbf{G}$) is selected from the permutations of the RCR $(\mathbf{H}\backslash)\mathbf{G}$, which has been described in

Theorem 1. Suppose that the permutation $p_g^{[R]}$ is represented by a cycle decomposition involving the number $\nu_d(p_g^{[R]})$ of d-cycles, where we place

$$\sum_{d=1}^{r} d\nu_d(p_g^{[R]}) = r = |\mathbf{G}|/|\mathbf{H}|. \tag{36}$$

Thus, the permutation $p_g^{[R]}$ possesses a cycle structure represented as follows:

$$1^{\nu_1(p_g^{[R]})} 2^{\nu_2(p_g^{[R]})} \dots d^{\nu_d(p_g^{[R]})} \dots r^{\nu_r(p_g^{[R]})}. \tag{37}$$

Let us consider the action of the permutation (eq. 37) on the **H**-segments (accommodating the proligands) in the stereoisomer. The action of the d-cycle of the permutation (eq. 37) varies in accord with the sphericity indices, which are originally determined on the sphericities of the orbits (cf. eqs. 22 and 25). To clarify this action, the concept "sphericities of orbits" into conceptually transformed into the concept "sphericities of cycles". This has been accomplished by using an intermediate concept "sphericities of the orbits of cyclic subgroups" in the original formulation of the proligand method [15, 16, 17]. In this paper, a more intuitive treatment will be developed as follows.

According to Fujita's proligand method [15, 16, 17], each d-cycle contained in the permutation $p_g^{[R]}$ is defined as follows:

1. **Hemispheric cycle:** When g is a proper rotation each d-cycle contained in the permutation $p_g^{[R]}$ (d is odd or even) is called *a hemispheric cycle*, to which a sphericity index a_d is assigned.

2. **Homospheric cycle:** When g is an improper rotation and the size d of a cycle contained in the permutation $p_g^{[R]}$ is odd, the d-cycle is called *a homospheric cycle*, to which a sphericity index a_d is assigned.

3. **Enantiospheric cycle:** When g is an improper rotation and the size d of a cycle contained in the permutation $p_g^{[R]}$ is even, the d-cycle is called *an enantiospheric cycle*, to which a sphericity index c_d is assigned.

4.2.2 Ligand Inventories of Three Kinds

The sphericities of cycles described above allow us to assign a product of sphericity indices to each permutation $p_g^{[R]}$ in accord with eqs. 36 and 37, i.e.,

$$\$_1^{\nu_1(p_g^{[R]})} \$_2^{\nu_2(p_g^{[R]})} \dots \$_d^{\nu_d(p_g^{[R]})} \dots \$_r^{\nu_r(p_g^{[R]})}, \tag{38}$$

where the symbol $\$_d$ indicates b_d for a hemispheric cycle, a_d for a homospheric cycle, or c_d for an enantiospheric cycle.

1. When a hemispheric d-cycle (characterized by b_d) acts on a set of d proligands, they should be of the same kind so as to be transitive under the action. In addition, the proligands can be achiral or chiral without any restriction, because the d-cycle is contained in a proper rotation. In other word, any set of achiral proligands, X_1^d, X_2^d, $\cdots$, or X_t^d; any set

of chiral proligands, p_1^d, p_2^d, $\cdots$, or p_u^d; or any set of enantiomeric proligands, $\overline{\mathrm{p}}_1^d$, $\overline{\mathrm{p}}_2^d$, $\cdots$, or $\overline{\mathrm{p}}_u^d$ can be permuted by the hemispheric d-cycle. The action on each d-membered set can be expressed by the following equation:

$$b_d = \mathrm{X}_1^d + \mathrm{X}_2^d + \cdots + \mathrm{X}_t^d + \mathrm{p}_1^d + \mathrm{p}_2^d + \cdots + \mathrm{p}_u^d + \overline{\mathrm{p}}_1^d + \overline{\mathrm{p}}_2^d + \cdots + \overline{\mathrm{p}}_u^d, \tag{39}$$

which is called *a ligand inventory for the hemispheric cycle*.

2. When a homospheric d-cycle (characterized by a_d) acts on a set of d proligands, they should be of the same kind so as to be transitive under the action. Because the d-cycle is contained in an improper rotation, the total achirality should be maintained during this action. If the proligands are chiral, the chirality of each of the proligands is altered into the opposite one. To maintain the total achirality, the pairwise compensation of the opposite chiralities should occur. However, such pairwise compensation is impossible because d is odd. Hence, only a set of achiral proligands, X_1^d, X_2^d, $\cdots$, or X_t^d is permitted by the homospheric d-cycle. The action on each d-membered set can be expressed by the following equation:

$$a_d = \mathrm{X}_1^d + \mathrm{X}_2^d + \cdots + \mathrm{X}_t^d, \tag{40}$$

which is called *a ligand inventory for the homospheric cycle*.

3. When an enantiospheric d-cycle (characterized by c_d) acts on a set of d proligands, the action should be concerned with a set of achiral ligands of the same kind or with a pairwise set which contains $d/2$ of chiral ligands of the same kind and $d/2$ of their enantiomeric ligands. It is easy to find that such a set of achiral ligands of the same kind is transitive under the action. As a result, a set of achiral proligands, X_1^d, X_2^d, $\cdots$, or X_t^d is permitted so as to maintain the total achirality, On the other hand, the pairwise set also maintains the total achirality, even if the chirality of each of the proligands is altered into the opposite one. Hence, a set of enantiomeric proligands, $\mathrm{p}_1^{d/2}\overline{\mathrm{p}}_1^{d/2}$, $\mathrm{p}_2^{d/2}\overline{\mathrm{p}}_2^{d/2}$, ..., or $\mathrm{p}_u^{d/2}\overline{\mathrm{p}}_u^{d/2}$ can be permuted by the enantiospheric d-cycle, where each set exhibits two modes of pairwise packing. The action on each d-membered set can be expressed by the following equation:

$$c_d = \mathrm{X}_1^d + \mathrm{X}_2^d + \cdots + \mathrm{X}_t^d + 2\mathrm{p}_1^{d/2}\overline{\mathrm{p}}_1^{d/2} + 2\mathrm{p}_2^{d/2}\overline{\mathrm{p}}_2^{d/2} + \cdots + 2\mathrm{p}_u^{d/2}\overline{\mathrm{p}}_u^{d/2}, \tag{41}$$

which is called *a ligand inventory for the enantiospheric cycle*.

The present ligand inventories are the same contents as defined otherwise in Fujita's proligand method [15, 16, 17].

4.2.3 Total Number of Fixed Assemblies

The inventory of each cycle described above is a generating function for giving the number of fixed points (assemblies) as the coefficient of the term W_θ (i.e., $1 \times \mathrm{X}^d$ etc.) if the cycle is isolated. Because a set of relevant cycles is contained in the permutation $p_g^{[R]}$ shown in eq. 38, the ligand inventories of three kinds should be introduced into every cycles contained in the permutation ($p_g^{[R]}$). Thus, after the introduction of the ligand inventories (eqs. 39, 40, and 41) into the product of sphericity indices (eq. 38), the resulting equation is expanded to produce a generating function. Thereby, the numbers of fixed points (assemblies) on the action of each $p_g^{[R]}$ are obtained as the coefficients of the terms W_θ (eq. 31) appearing in the generating function.

When g runs over $\mathbf{G}$ in the form of the right coset representation $(\mathbf{H}\backslash)\mathbf{G}$ (or more generally eq. 28), the respective products (eq. 38) are summed up after the introduction of the ligand inventories so as to give the generating function:

$$\sum_{g\in\mathbf{G}} \$_1^{\nu_1(p_g^{[R]})}\$_2^{\nu_2(p_g^{[R]})}\cdots\$_d^{\nu_d(p_g^{[R]})}\cdots\$_r^{\nu_r(p_g^{[R]})}, \tag{42}$$

where each sphericity index $\$_d$ (a_d, b_d, or c_d) is replaced by the ligand inventories shown in eq. 39, 40, or 41. The expansion of eq. 42 produces a generating function, in which the total number of fixed assemblies for each molecular formula appears as the coefficient of the corresponding term W_θ (eq. 31).

4.3 Fujita's Proligand Method

4.3.1 Enumeration of Achiral plus Chiral Stereoisomers

The total number of fixed assemblies calculated from the numbers of fixed assemblies *per stereoisomer* (eq. 35) is equal to the total number of fixed assemblies calculated from the numbers of fixed assemblies *per permutation* (eq. 42), because they are simply different in the orders of summation. Hence, the equalization of eq. 35 with eq. 42 and the subsequent division by $|\mathbf{G}|$ give the following generating function:

$$\sum_{[\theta]} B_\theta W_\theta = \frac{1}{|\mathbf{G}|}\sum_{g\in\mathbf{G}} \$_1^{\nu_1(p_g^{[R]})}\$_2^{\nu_2(p_g^{[R]})}\cdots\$_d^{\nu_d(p_g^{[R]})}\cdots\$_r^{\nu_r(p_g^{[R]})}, \tag{43}$$

where the term W_θ is represented by eq. 31, the sum in the left-hand side is concerned with the partition $[\theta]$ (eq. 30), and each sphericity index $\$_d$ ($= a_d$, b_d, or c_d) in the right-hand side is replaced by the ligand inventories shown in eq. 39, 40, or 41.

The result shown in eq. 43 can be written in a more succinct manner by defining a cycle index with chirality fittingness (CI-CF) as follows:

$$\text{CI-CF}(\mathbf{G},\$_d) = \frac{1}{|\mathbf{G}|}\sum_{g\in\mathbf{G}} \$_1^{\nu_1(p_g^{[R]})}\$_2^{\nu_2(p_g^{[R]})}\cdots\$_d^{\nu_d(p_g^{[R]})}\cdots\$_r^{\nu_r(p_g^{[R]})} \tag{44}$$

which has the same form as the right-hand side of eq. 43 but has not been substituted by the ligand inventories. For cases in which $\mathbf{H}$ of the $(\mathbf{H}\backslash)\mathbf{G}$ moves on the subgroups of $\mathbf{G}$ so as to construct two or more orbits, the CI-CF (eq. 44) should be expressed on the basis of eq. 28.

The discussions described above are summarized as a theorem:

Theorem 2 (Enumeration of Achiral Plus Chiral Stereoisomers) Suppose that the positions of a given skeleton of $\mathbf{G}$-symmetry accommodate achiral and chiral proligands selected from $\mathbf{X}$ (eq. 29), where each operation of $\mathbf{G}$ acting on the positions is represented by the cycle structure shown in eq. 37 and the product of sphericity indices shown in eq. 38. Let B_θ be the number of non-equivalent stereoisomers having the molecular formula W_θ (eq. 31), where the partition $[\theta]$ is represented by eq. 30. The numbers B_θ appear as the coefficients in a generating function represented as follows:

$$\sum_{[\theta]} B_\theta W_\theta = \text{CI-CF}(\mathbf{G},\$_d), \tag{45}$$

where the sphericity indices $\$_d$ (a_d, b_d, or c_d) in the CI-CF (eq. 44) are replaced by the ligand inventories shown in eqs. 39, 40, and 41. □

Table 1: Right Coset Representation $(\mathbf{C}_s\backslash)\mathbf{D}_{2d}$ and Products of Sphericity Indices.[a]

symmetry operation		RCR $(\mathbf{C}_s\backslash)\mathbf{D}_{2d}$ as product of cycles	product of sphericity indices	product of dummy variables
I	$\sim$	$(1)(2)(3)(4)$	b_1^4	s_1^4
$C_{2(1)}$	$\sim$	$(1\,2)(3\,4)$	b_2^2	s_2^2
$C_{2(2)}$	$\sim$	$(1\,4)(2\,3)$	b_2^2	s_2^2
$C_{2(3)}$	$\sim$	$(1\,3)(2\,4)$	b_2^2	s_2^2
$\sigma_{d(1)}$	$\sim$	$\overline{(1)(2\,4)(3)}$	$a_1^2c_2$	$s_1^2s_2$
S_4	$\sim$	$\overline{(1\,2\,3\,4)}$	c_4	s_4
S_4^3	$\sim$	$\overline{(1\,4\,3\,2)}$	c_4	s_4
$\sigma_{d(2)}$	$\sim$	$\overline{(1\,3)(2)(4)}$	$a_1^2c_2$	$s_1^2s_2$

[a] Each cycle appearing in an improper rotation is designated by an overbar, which represents the inversion of ligand chirality.

Although the product of sphericity indices (eq. 38) is concerned with the RCR $(\mathbf{H}\backslash)\mathbf{G}$, it is easy to obtain the product of sphericity indices for general cases, where the product (eq. 38) corresponds to the sum of RCRs shown in eq. 28. Moreover, the set $\mathbf{X}$ (eq. 29) is allowed to be different according to each of the RCRs (eq. 28). Thereby, Theorem 2 can be easily extended to satisfy such general cases.

Example 1. Let us now examine stereoisomer enumeration based on an allene skeleton (cf. Figs. 8 and 13) by means of Theorem 2. The four positions of the allene skeleton are governed by the RCR $(\mathbf{C}_s\backslash)\mathbf{D}_{2d}$ shown in eqs. 4–11. According to the cycle structure of each permutation, the corresponding product of sphericity indices is calculated, as shown in Table 1. Hence, the CI-CF for this case is obtained by means of eq. 44 as follows:

$$\text{CI-CF}(\mathbf{D}_{2d},\$_d) = \frac{1}{8}\left(b_1^4+3b_2^2+2a_1^2c_2+2c_2^2\right). \tag{46}$$

Obviously, eq. 46 is identical with eq. 75 of Part 3 [3], which has been alternatively obtained by the CI (cycle-index) method of Fujita's USCI approach.

Suppose that a set of four proligands selected from the set:

$$\mathbf{X} = \{\mathrm{H},\mathrm{X},\mathrm{p},\overline{\mathrm{p}}\} \tag{47}$$

is placed on the allene skeleton. In accord with the set $\mathbf{X}$ for this case, the partition $[\theta]$ (eq. 30) is calculated to be

$$[\theta] : h+x+p+\overline{p} = 4, \tag{48}$$

where the letters in the right-hand side represent non-negative integers. The molecular formula W_θ (eq. 31) is calculated as follows:

$$W_\theta = \mathrm{H}^h\mathrm{X}^x\mathrm{p}^p\overline{\mathrm{p}}^{\overline{p}} \tag{49}$$

For chiral stereoisomers, a molecular formula W_θ due to eq. 32 should be used as follows:

$$W_\theta = \frac{1}{2}\left(\mathrm{H}^h\mathrm{X}^x\mathrm{p}^p\overline{\mathrm{p}}^{\overline{p}}+\mathrm{H}^h\mathrm{X}^x\mathrm{p}^{\overline{p}}\overline{\mathrm{p}}^{p}\right). \tag{50}$$

According to Theorem 2, the ligand inventories (eqs. 39, 40, and 41) are obtained for this case as follows:

$$b_d = \mathrm{H}^d + \mathrm{X}^d + \mathrm{p}^d + \overline{\mathrm{p}}^d \tag{51}$$

$$a_d = \mathrm{H}^d + \mathrm{X}^d \tag{52}$$

$$c_d = \mathrm{H}^d + \mathrm{X}^d + 2\mathrm{p}^{d/2}\overline{\mathrm{p}}^{d/2}. \tag{53}$$

These inventories (eqs. 51–53) are introduced into the CI-CF (eq. 46) to give the following generating function:

$$\begin{aligned}
\sum_{[\theta]} B_\theta W_\theta \;=\; & (\mathrm{H}^4 + \mathrm{X}^4) + (\mathrm{H}^3\mathrm{X} + \mathrm{H}\mathrm{X}^3) + 2\mathrm{H}^2\mathrm{X}^2 \\
& + \frac{1}{2}(\mathrm{H}^3\mathrm{p} + \mathrm{H}^3\overline{\mathrm{p}}) + \frac{1}{2}(\mathrm{X}^3\mathrm{p} + \mathrm{X}^3\overline{\mathrm{p}}) \\
& + 3\times\frac{1}{2}(\mathrm{H}^2\mathrm{X}\mathrm{p} + \mathrm{H}^2\mathrm{X}\overline{\mathrm{p}}) + 3\times\frac{1}{2}(\mathrm{H}\mathrm{X}^2\mathrm{p} + \mathrm{H}\mathrm{X}^2\overline{\mathrm{p}}) \\
& + 3\times\frac{1}{2}(\mathrm{H}^2\mathrm{p}^2 + \mathrm{H}^2\overline{\mathrm{p}}^2) + 3\times\frac{1}{2}(\mathrm{X}^2\mathrm{p}^2 + \mathrm{X}^2\overline{\mathrm{p}}^2) + 3\times\frac{1}{2}(\mathrm{H}\mathrm{X}\mathrm{p}^2 + \mathrm{H}\mathrm{X}\overline{\mathrm{p}}^2) \\
& + (2\mathrm{H}^2\mathrm{p}\overline{\mathrm{p}} + 2\mathrm{X}^2\mathrm{p}\overline{\mathrm{p}}) + 4\mathrm{H}\mathrm{X}\mathrm{p}\overline{\mathrm{p}} \\
& + 3\times\frac{1}{2}(\mathrm{H}\mathrm{p}^2\overline{\mathrm{p}} + \mathrm{H}\mathrm{p}\overline{\mathrm{p}}^2) + 3\times\frac{1}{2}(\mathrm{X}\mathrm{p}^2\overline{\mathrm{p}} + \mathrm{X}\mathrm{p}\overline{\mathrm{p}}^2) \\
& + \frac{1}{2}(\mathrm{H}\mathrm{p}^3 + \mathrm{H}\overline{\mathrm{p}}^3) + \frac{1}{2}(\mathrm{X}\mathrm{p}^3 + \mathrm{X}\overline{\mathrm{p}}^3) \\
& + 2\mathrm{p}^2\overline{\mathrm{p}}^2 + \frac{1}{2}(\mathrm{p}^3\overline{\mathrm{p}} + \mathrm{p}\overline{\mathrm{p}}^3) + \frac{1}{2}(\mathrm{p}^4 + \overline{\mathrm{p}}^4).
\end{aligned} \tag{54}$$

The coefficient of each term (or each combined term) represents the total number of stereoisomers with the corresponding weight (molecular formula). This generating function is identical with eq. 76 of Part 3 [3], which has been alternatively obtained by the CI (cycle-index) method of the diagrammatical version (Part 3) of Fujita's USCI approach [4].

To verify the results shown in the generating function (eq. 54), let us examine the coefficient 4 of the term $\mathrm{HXp}\overline{\mathrm{p}}$, which means the existence of four stereoisomers of the molecular formula $\mathrm{HXp}\overline{\mathrm{p}}$. Among them, two achiral stereoisomers have been already depicted in Fig. 12, i.e., **60** and **61**. In addition, there exist two pairs of enantiomers, i.e., **116/$\overline{\mathbf{116}}$** and **117/$\overline{\mathbf{117}}$**, as shown in Fig. 20. Thus, the existence of the two achiral stereoisomers and the two pairs of the enantiomers is in agreement with the coefficient 4 of the term $\mathrm{HXp}\overline{\mathrm{p}}$ in the generating function (eq. 54).

Strictly speaking, eq. 50 should be used to represent the molecular formula of the pair **116/$\overline{\mathbf{116}}$** (or **117/$\overline{\mathbf{117}}$**). Because H (or X) is achiral, the H (or X) is identical with its hypothetical enantiomeric form $\overline{\mathrm{H}}$ (or $\overline{\mathrm{X}}$), i.e., $\mathrm{H} = \overline{\mathrm{H}}$ (or $\mathrm{X} = \overline{\mathrm{X}}$). For the chiral ligands p and $\overline{\mathrm{p}}$, we can place $\overline{\overline{\mathrm{p}}} = \mathrm{p}$. Hence, eq. 50 for this case is calculated as follows:

$$\frac{1}{2}\left(\mathrm{HXp}\overline{\mathrm{p}} + \overline{\mathrm{HX}\overline{\mathrm{p}}\overline{\mathrm{p}}}\right) = \mathrm{HXp}\overline{\mathrm{p}}, \tag{55}$$

where the right-hand side apparently belongs to the form of eq. 49. □

4.3.2 Enumeration of Achiral Stereoisomers

By means of Theorem 2, stereoisomer enumeration due to an achiral skeleton of **G** can be conducted to count the number of achiral stereoisomers plus the number of pairs of enantiomers.

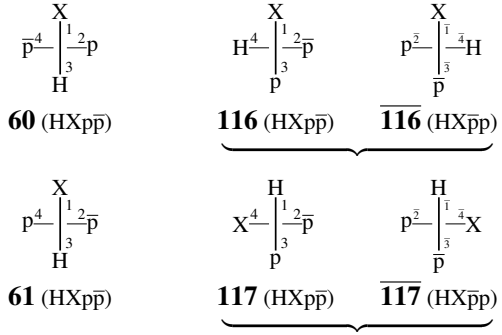

Figure 20: Two achiral stereoisomers and two pairs of enantiomers which have the molecular formula HXp$\overline{\text{p}}$.

Let us now consider the maximum chiral subgroup $\mathbf{G}'$ of the group $\mathbf{G}$ in accord with the treatment described in Ref. [16]. Under the group $\mathbf{G}'$, each chiral stereoisomer and its enantiomer are counted separately as distinct two stereoisomers, where they are counted pairwise as one stereoisomer under $\mathbf{G}$ as described above.

Let B'_θ be the number of stereoisomers where an achiral stereoisomer is counted once, while a chiral stereoisomer and its enantiomer are counted separately. To evaluate B'_θ, the terms corresponding to the subgroup $\mathbf{G}'$ are selected from eq. 44 to give the following CI-CF:

$$\text{CI-CF}(\mathbf{G}', b_d) = \frac{1}{|\mathbf{G}'|} \sum_{g \in \mathbf{G}'} b_1^{\nu_1(p_g^{[R]})} b_2^{\nu_2(p_g^{[R]})} \cdots b_d^{\nu_d(p_g^{[R]})} \cdots b_r^{\nu_r(p_g^{[R]})}, \tag{56}$$

where only hemispheric indices remain and $|\mathbf{G}'| = |\mathbf{G}|/2$. Let us replace the CI-CF in eq. 44 by the CI-CF in eq. 56 so as to give the following equation:

$$\sum_{[\theta]} B'_\theta W_\theta = \text{CI-CF}(\mathbf{G}', b_d). \tag{57}$$

On the same line as Theorem 2, a generating function for calculating the number of stereoisomers B'_θ is obtained by introducing the ligand inventory (shown in eq. 39) into the sphericity index b_d of eq. 57.

Let the symbols N_A and N_C represent generating functions for calculating the numbers of achiral stereoisomers and the numbers of enantiomeric pairs of chiral stereoisomers. Then, the left-hand side of eq. 57 means that

$$\sum_{[\theta]} B'_\theta W_\theta = N_A + 2N_C, \tag{58}$$

while the left-hand side of eq. 45 means that

$$\sum_{[\theta]} B_\theta W_\theta = N_A + N_C. \tag{59}$$

Hence, N_A and N_C are calculated as follows:

$$N_A = 2\sum_{[\theta]} B_\theta W_\theta - \sum_{[\theta]} B'_\theta W_\theta = 2\text{CI-CF}(\mathbf{G}, \$_d) - \text{CI-CF}(\mathbf{G}', b_d) \tag{60}$$

$$N_C = \sum_{[\theta]} B'_\theta W_\theta - \sum_{[\theta]} B_\theta W_\theta = \text{CI-CF}(\mathbf{G}', b_d) - \text{CI-CF}(\mathbf{G}, \$_d), \tag{61}$$

where eq. 45 and eq. 57 are used. The sphericity indices $\$_d$ (i.e., a_d, b_d, or c_d) in the CI-CFs (eqs. 60 and 61) are replaced by the ligand inventories shown in eqs. 39, 40, and 41.

When the terms $2B_\theta$ (cf. eqs. 43 and 44) and B'_θ (cf. eqs. 56 and 57) are concerned with an enantiomeric pair of chiral stereoisomers characterized by the partition $[\theta]$, the term $2B_\theta$ corresponds to the term:

$$2B_\theta \times \frac{1}{2}\left\{[\mathrm{X}_1^{\theta_1}\cdots\mathrm{p}_1^{\theta'_1}\cdots\overline{\mathrm{p}}_1^{\theta''_1}\cdots] + [\mathrm{X}_1^{\theta_1}\cdots\mathrm{p}_1^{\theta''_1}\cdots\overline{\mathrm{p}}_1^{\theta'_1}\cdots]\right\} \tag{62}$$

by means of eq. 32, while the term B'_θ corresponds to the term:

$$B'_\theta \times \left\{[\mathrm{X}_1^{\theta_1}\cdots\mathrm{p}_1^{\theta'_1}\cdots\overline{\mathrm{p}}_1^{\theta''_1}\cdots] + [\mathrm{X}_1^{\theta_1}\cdots\mathrm{p}_1^{\theta''_1}\cdots\overline{\mathrm{p}}_1^{\theta'_1}\cdots]\right\}, \tag{63}$$

because two stereoisomers of the enantiomeric pair are counted separately under $\mathbf{G}'$. They are equal to each other so that we obtain $2B_\theta W_\theta - B'_\theta W_\theta = 0$ for each pair of enantiomeric stereoisomers. This means that the remaining terms in the N_A (eq. 60) are concerned with improper rotations only. On condition that the molecular formulas W_θ for chiral stereoisomers (in eqs. 60 and 61) are treated as above to adjust the summation in $\sum_{[\theta]} B_\theta W_\theta$ to be consistent to the summation in $\sum_{[\theta]} B'_\theta W_\theta$, the coefficient $2B_\theta - B'_\theta$ ($= A_\theta$) appears in eq. 60 for counting achiral stereoisomers, while the coefficient $B'_\theta - B_\theta$ ($= C_\theta$) appears eq. 61.

As a result of the discussion in the preceding paragraph on the summations in eq. 60, the right-hand side of eq. 60 can be transformed into a more concrete format. Because of the relationship $|\mathbf{G}'| = |\mathbf{G}|/2$, the twice of the CI-CF$(\mathbf{G}, \$_d)$ (eq. 44) contains the whole of CI-CF$(\mathbf{G}', b_d)$ (eq. 56) once so that all of the terms for proper rotations are deleted from the twice of CI-CF$(\mathbf{G}, b_d)$. By placing $\overline{\mathbf{G}} = \mathbf{G} - \mathbf{G}'$, we can define the CI-CF$_A$ as follows:

$$N_A = \text{CI-CF}_A(\overline{\mathbf{G}}, \$_d) = \frac{1}{|\overline{\mathbf{G}}|}\sum_{g\in\overline{\mathbf{G}}} \$_1^{\nu_1(p_g^{[R]})}\$_2^{\nu_2(p_g^{[R]})}\cdots\$_d^{\nu_d(p_g^{[R]})}\cdots\$_r^{\nu_r(p_g^{[R]})}, \tag{64}$$

where the sphericity indices $\$_d$ are a_d or c_d and all of the terms bearing b_d disappear. Note that the summation is concerned with improper rotations $g \in \overline{\mathbf{G}}$ ($= \mathbf{G} - \mathbf{G}'$) and the divisor is equal to $|\overline{\mathbf{G}}| = |\mathbf{G}|/2$.

By employing eq. 64, the numbers of achiral stereoisomers A_θ are calculated according to the following theorem:

Theorem 3 (Enumeration of Achiral Stereoisomers) Let the symbol A_θ be the number of non-equivalent achiral stereoisomers having the molecular formula W_θ, where the same conditions of Theorem 2 are postulated. Then, the numbers of non-equivalent achiral stereoisomers A_θ appear as the coefficients in a generating function represented as follows:

$$\sum_{[\theta]} A_\theta W_\theta = \text{CI-CF}_A(\overline{\mathbf{G}}, \$_d) \tag{65}$$

where the sphericity indices $\$_d$ (a_d and c_d) in the CI-CF$_A$ (eq. 64) are replaced by the ligand inventories shown in eqs. 40 and 41. □

Example 2. As a continuation of Example 1, let us obtain the numbers (A_θ) of achiral stereoisomers among the total numbers of achiral plus chiral stereoisomers. The CI-CF$_A(\overline{\mathbf{D}_{2d}}, \$_d)$ is obtained by applying eq. 64 to this case:

$$\text{CI-CF}_A(\overline{\mathbf{D}_{2d}}, \$_d) = \frac{1}{4}(2a_1^2c_2 + 2c_4) = \frac{1}{2}a_1^2c_2 + \frac{1}{2}c_4, \tag{66}$$

where the products of sphericity indices for the improper rotations are collected from Table 1. By following Theorem 2, the ligand inventories (eqs. 52 and 53) are introduced to eq. 66. The resulting equation is expanded to give a generating function:

$$\begin{aligned}\sum_{[\theta]} A_\theta W_\theta &= (\mathrm{H}^4 + \mathrm{X}^4) + (\mathrm{H}^3\mathrm{X} + \mathrm{H}\mathrm{X}^3) + \mathrm{H}^2\mathrm{X}^2 \\ &\quad + (\mathrm{H}^2\mathrm{p}\overline{\mathrm{p}} + \mathrm{X}^2\mathrm{p}\overline{\mathrm{p}}) + 2\mathrm{H}\mathrm{X}\mathrm{p}\overline{\mathrm{p}} + \mathrm{p}^2\overline{\mathrm{p}}^2 \end{aligned} \tag{67}$$

The coefficient 2 of the term HXp$\overline{\text{p}}$ in eq. 67 indicates the existence of two achiral stereoisomers of the molecular formula HXp$\overline{\text{p}}$. The two achiral stereoisomers have been already examined in Fig. 20, i.e., **60** and **61**. □

4.3.3 Enumeration of Chiral Stereoisomers

The term CI-CF$(\mathbf{G}, \$_d)$ is deleted from eq. 60 and eq. 61 to give

$$N_A + 2N_C = \text{CI-CF}_A(\mathbf{G}', b_d), \tag{68}$$

which is essentially equivalent to eq. 58. By introducing N_A (eq. 64) into eq. 68, we can derive the generating function N_C for calculating the numbers of chiral stereoisomers (enantiomeric pairs), i.e.,

$$N_C = \frac{1}{2}\left(\text{CI-CF}(\mathbf{G}', b_d) - N_A\right) = \frac{1}{2}\text{CI-CF}(\mathbf{G}', b_d) - \frac{1}{2}\text{CI-CF}_A(\overline{\mathbf{G}}, \$_d) \tag{69}$$

By introducing eqs. 56 and 64 into eq. 69 (note that $|\mathbf{G}'| = |\overline{\mathbf{G}}| = |\mathbf{G}|/2$), we can define the CI-CF$_C$ as follows:

$$\begin{aligned} N_C &= \text{CI-CF}_C(\mathbf{G}, \$_d) \\ &= \frac{1}{|\mathbf{G}|}\left\{ \sum_{g \in \mathbf{G}'} b_1^{\nu_1(p_g^{[R]})} b_2^{\nu_2(p_g^{[R]})} \cdots b_d^{\nu_d(p_g^{[R]})} \cdots b_r^{\nu_r(p_g^{[R]})} \right. \\ &\qquad \left. - \sum_{g \in \overline{\mathbf{G}}} \$_1^{\nu_1(p_g^{[R]})} \$_2^{\nu_2(p_g^{[R]})} \cdots \$_d^{\nu_d(p_g^{[R]})} \cdots \$_r^{\nu_r(p_g^{[R]})} \right\}, \end{aligned} \tag{70}$$

where the sphericity indices $\$_d$ in the latter summation are a_d or c_d. It should be noted that the first summation is concerned with proper rotations $g \in \mathbf{G}'$; and that the second summation is concerned with improper rotations $g \in \overline{\mathbf{G}}$ $(= \mathbf{G} - \mathbf{G}')$. The comparison of the CI-CF$_C$ (eq. 70) with the CI-CF (eq. 44) reveals that the plus signs of the terms for the improper rotations appearing in eq. 44 are simply changed into minus signs so as to generate eq. 70. By using eq. 70, the numbers of achiral stereoisomers C_θ are calculated according to the following theorem:

Theorem 4 (Enumeration of Chiral Stereoisomers as Pairs of Enantiomers) Let the symbol C_θ be the number of non-equivalent pairs of enantiomers having the molecular formula W_θ, where the same conditions of Theorem 2 are postulated. The numbers of chiral stereoisomers C_θ appear as the coefficients in a generating function represented as follows:

$$\sum_{[\theta]} C_\theta W_\theta = \text{CI-CF}_C(\mathbf{G}, \$_d) \tag{71}$$

where the sphericity indices $\$_d$ (b_d, a_d, or c_d) in the CI-CF$_C$ (eq. 70) are replaced by the ligand inventories shown in eqs. 39, 40 and 41. □

Example 3. As a continuation of Examples 1 and 2, let us obtain the numbers (C_θ) of enantiomeric pairs of chiral stereoisomers among the total numbers of achiral plus chiral stereoisomers. The CI-CF$_C(\mathbf{D}_{2d}, \$_d)$ is obtained by applying eq. 70 to this case:

$$\text{CI-CF}_C(\mathbf{D}_{2d}, \$_d) = \frac{1}{8}\left(b_1^4 + 3b_2^2 - 2a_1^2c_2 - 2c_2^2\right). \tag{72}$$

where the plus sign of the term for each improper rotation in eq. 46 is changed into minus. By following Theorem 4, the ligand inventories (eqs. 51–53) are introduced into eq. 72. The resulting equation is expanded to give a generating function:

$$\begin{aligned}
\sum_{[\theta]} C_\theta W_\theta \;=\; & \mathrm{H}^2\mathrm{X}^2 \\
& + \frac{1}{2}(\mathrm{H}^3\mathrm{p} + \mathrm{H}^3\overline{\mathrm{p}}) + \frac{1}{2}(\mathrm{X}^3\mathrm{p} + \mathrm{X}^3\overline{\mathrm{p}}) \\
& + 3 \times \frac{1}{2}(\mathrm{H}^2\mathrm{Xp} + \mathrm{H}^2\mathrm{X}\overline{\mathrm{p}}) + 3 \times \frac{1}{2}(\mathrm{HX}^2\mathrm{p} + \mathrm{HX}^2\overline{\mathrm{p}}) \\
& + 3 \times \frac{1}{2}(\mathrm{H}^2\mathrm{p}^2 + \mathrm{H}^2\overline{\mathrm{p}}^2) + 3 \times \frac{1}{2}(\mathrm{X}^2\mathrm{p}^2 + \mathrm{X}^2\overline{\mathrm{p}}^2) + 3 \times \frac{1}{2}(\mathrm{HXp}^2 + \mathrm{HX}\overline{\mathrm{p}}^2) \\
& + (\mathrm{H}^2\mathrm{p}\overline{\mathrm{p}} + \mathrm{X}^2\mathrm{p}\overline{\mathrm{p}}) + 2\mathrm{HXp}\overline{\mathrm{p}} \\
& + 3 \times \frac{1}{2}(\mathrm{Hp}^2\overline{\mathrm{p}} + \mathrm{Hp}\overline{\mathrm{p}}^2) + 3 \times \frac{1}{2}(\mathrm{Xp}^2\overline{\mathrm{p}} + \mathrm{Xp}\overline{\mathrm{p}}^2) \\
& + \frac{1}{2}(\mathrm{Hp}^3 + \mathrm{H}\overline{\mathrm{p}}^3) + \frac{1}{2}(\mathrm{Xp}^3 + \mathrm{X}\overline{\mathrm{p}}^3) \\
& + \mathrm{p}^2\overline{\mathrm{p}}^2 + \frac{1}{2}(\mathrm{p}^3\overline{\mathrm{p}} + \mathrm{p}\overline{\mathrm{p}}^3) + \frac{1}{2}(\mathrm{p}^4 + \overline{\mathrm{p}}^4).
\end{aligned} \tag{73}$$

The coefficient 2 of the term HXp$\overline{\text{p}}$ in eq. 73 indicates that there exist two pairs of enantiomers of the molecular formula HXp$\overline{\text{p}}$. The two pairs of enantiomers have been already depicted in Fig. 20, i.e., **116/$\overline{\mathbf{116}}$** and **117/$\overline{\mathbf{117}}$**. □

5 Comparison of Theorem 2 with Pólya's Theorem

5.1 Deficiency of Pólya's Theorem in Stereoisomer Enumeration

Pólya's Theorem has presumed that objects placed on a skeleton are structureless [12], as discussed in Introduction. This presumption causes the deficiency of Pólya's theorem in stereoisomer enumeration, where pseudoasymmetric cases cannot be treated properly. This type of deficiency shall be examined by using the same subject as discussed Examples 1 to 3.

Example 4. A conventional way of stereoisomer enumeration according to Pólya's Theorem is based on the usage of the maximum chiral subgroup, as shown in several textbooks [23, 12]. By starting from the data shown in Table 1, we obtain Pólya's cycle index as follows:

$$\mathrm{CI}(\mathbf{D}, s_d) = \frac{1}{4}\left(s_1^4 + 3s_2^2\right), \tag{74}$$

which contains dummy variables in place of sphericity indices. The set $\mathbf{X}$ (eq. 47) and the partition $[\theta]$ (eq. 48 are also used. However, eq. 50 for a pair of enantiomers is not used, and the molecular formula W_θ (eq. 49) is used separately to characterize the two enantiomers of the pair. As a result, the following ligand inventory of one kind is used:

$$s_d = \mathrm{H}^d + \mathrm{X}^d + \mathrm{p}^d + \overline{\mathrm{p}}^d. \tag{75}$$

This inventory (eqs. 75) is introduced into the Pólya's CI (eq. 74). The resulting equation is expanded to give the following generating function:

$$\begin{aligned} f_{\mathbf{D}_2} \;=\; & (\mathrm{H}^4 + \mathrm{X}^4) + (\mathrm{H}^3\mathrm{X} + \mathrm{H}\mathrm{X}^3) + 3\mathrm{H}^2\mathrm{X}^2 \\ & + (\mathrm{H}^3\mathrm{p} + \mathrm{H}^3\overline{\mathrm{p}}) + (\mathrm{X}^3\mathrm{p} + \mathrm{X}^3\overline{\mathrm{p}}) \\ & + (3\mathrm{H}^2\mathrm{X}\mathrm{p} + 3\mathrm{H}^2\mathrm{X}\overline{\mathrm{p}}) + (3\mathrm{H}\mathrm{X}^2\mathrm{p} + 3\mathrm{H}\mathrm{X}^2\overline{\mathrm{p}}) \\ & + (3\mathrm{H}^2\mathrm{p}^2 + 3\mathrm{H}^2\overline{\mathrm{p}}^2) + (3\mathrm{X}^2\mathrm{p}^2 + 3\mathrm{X}^2\overline{\mathrm{p}}^2) + (3\mathrm{H}\mathrm{X}\mathrm{p}^2 + 3\mathrm{H}\mathrm{X}\overline{\mathrm{p}}^2) \\ & + (3\mathrm{H}^2\mathrm{p}\overline{\mathrm{p}} + 3\mathrm{X}^2\mathrm{p}\overline{\mathrm{p}}) + 6\mathrm{H}\mathrm{X}\mathrm{p}\overline{\mathrm{p}} \\ & + (3\mathrm{H}\mathrm{p}^2\overline{\mathrm{p}} + 3\mathrm{H}\mathrm{p}\overline{\mathrm{p}}^2) + (3\mathrm{X}\mathrm{p}^2\overline{\mathrm{p}} + 3\mathrm{X}\mathrm{p}\overline{\mathrm{p}}^2) \\ & + (\mathrm{H}\mathrm{p}^3 + \mathrm{H}\overline{\mathrm{p}}^3) + (\mathrm{X}\mathrm{p}^3 + \mathrm{X}\overline{\mathrm{p}}^3) \\ & + 3\mathrm{p}^2\overline{\mathrm{p}}^2 + (\mathrm{p}^3\overline{\mathrm{p}} + \mathrm{p}\overline{\mathrm{p}}^3) + (\mathrm{p}^4 + \overline{\mathrm{p}}^4). \end{aligned} \tag{76}$$

The coefficient 6 of the term $\mathrm{HXp}\overline{\mathrm{p}}$ in eq. 76 indicates that there exist six stereoisomers of the molecular formula $\mathrm{HXp}\overline{\mathrm{p}}$ under the enumeration based on Pólya's theorem. Thus, the six stereoisomers listed in Fig. 20, i.e., **60**, **61**, **116**, $\overline{\mathbf{116}}$, **117**, and $\overline{\mathbf{117}}$, are counted separately so that the achirality of **60** (or **61**), the chirality of the remaining four stereoisomers, and the enantiomeric relationship between **116** and $\overline{\mathbf{116}}$ (or between **117** and $\overline{\mathbf{117}}$) are disregarded thoroughly. □

To characterize such achirality as disregarded in Example 4, the conventional way due to Pólya's Theorem uses the full operations of $\mathbf{D}_{2d}$, where objects placed on a skeleton are regarded as being structureless. This methodology has been described in the textbook written by Pólya et al. [12]. In the next example, let us demonstrate that the methodology is permitted only to treat such structureless objects.

Example 5. By starting from the data shown in Table 1, the use of $\mathbf{D}_{2d}$ gives Pólya's cycle index as follows:

$$\mathrm{CI}(\mathbf{D}_{2d}, s_d) = \frac{1}{8}\left(s_1^4 + 3s_2^2 + 2s_1^2 s_2 + 2s_2^2\right). \tag{77}$$

The inventory (eqs. 75) is introduced into the Pólya's CI (eq. 77). The resulting equation is expanded to give the following generating function:

$$\begin{aligned} f_{\mathbf{D}_{2d}} \;=\; & (\mathrm{H}^4 + \mathrm{X}^4) + (\mathrm{H}^3\mathrm{X} + \mathrm{H}\mathrm{X}^3) + 2\mathrm{H}^2\mathrm{X}^2 \\ & + (\mathrm{H}^3\mathrm{p} + \mathrm{H}^3\overline{\mathrm{p}}) + (\mathrm{X}^3\mathrm{p} + \mathrm{X}^3\overline{\mathrm{p}}) \\ & + (2\mathrm{H}^2\mathrm{X}\mathrm{p} + 2\mathrm{H}^2\mathrm{X}\overline{\mathrm{p}}) + (2\mathrm{H}\mathrm{X}^2\mathrm{p} + 2\mathrm{H}\mathrm{X}^2\overline{\mathrm{p}}) \end{aligned}$$

$$
\begin{aligned}
&+(2H^2p^2+2H^2\overline{p}^2)+(2X^2p^2+2X^2\overline{p}^2)+(2HXp^2+2HX\overline{p}^2)\\
&+(2H^2p\overline{p}+2X^2p\overline{p})+3HXp\overline{p}\\
&+(2Hp^2\overline{p}+2Hp\overline{p}^2)+(2Xp^2\overline{p}+2Xp\overline{p}^2)\\
&+(Hp^3+H\overline{p}^3)+(Xp^3+X\overline{p}^3)\\
&+2p^2\overline{p}^2+(p^3\overline{p}+p\overline{p}^3)+(p^4+\overline{p}^4).
\end{aligned}
\tag{78}
$$

The coefficient 3 of the term $HXp\overline{p}$ in eq. 78 indicates that there exist three stereoisomers of the molecular formula $HXp\overline{p}$ under the enumeration based on Pólya's theorem. Thus, the six stereoisomers listed in Fig. 20 are categorized into three pairs: a pair of **60/61**, a pair of **116/$\overline{116}$**, and a pair of **117/$\overline{117}$**, each of which is counted once under the Pólya's theorem using $\mathbf{D}_{2d}$. Obviously, the two stereoisomers (**60** and **61**) of the first pair are diastereomeric, while the two of the second or third pair are enantiomeric. It follows that the diastereomeric relationship is not discriminated from the enantiomeric relationship. Moreover, the two stereoisomers (**60** and **61**) should be counted as distinct stereoisomers because they are diastereomeric from the stereochemical point of view. Note that, if the proligand p and $\overline{p}$ in **60** and **61** are replaced by achiral proligands Y and Z, the resulting stereoisomers of HXYZ are enantiomeric to each other. Hence the diastereomeric pair can be regarded as a kind of pseudoasymmetric case. The enumeration procedure due to Pólya's theorem has failed in characterization of such a pseudoasymmetry case. □

5.2 Prismane Derivatives

In connection with the number of derivatives of benzene (C_6H_6), Pólya et al. have once enumerated isomeric derivatives based on a prismane skeleton (C_6H_6) in Chapter 6 of their textbook [12]. Because their purpose was to prove the hexagonal structure of the benzene nucleus, it was natural to limit substituents to atoms (or achiral ligands). In fact, Pólya's theorem worked well under this limitation only, even though enumeration of stereoisomers was claimed to be fulfilled without mentioning such limitation [24].

Stereochemistry, however, has taken account of chiral ligands as well as achiral ones (or atoms) from its beginning by van't Hoff [25, 26], where *meso*-compounds and pseudoasymmetry in stereoisomerism have been concerned with the presence of chiral ligands in molecules. It is permitted to say that chemical applications of Pólya's theorem have still remained in the stage before the beginning of stereochemistry, because there have been no attempts to apply Pólya's theorem to cases in which chiral ligands as well as achiral ones (or atoms) are considered as substituents.

In this subsection, the same problem as discussed in the Pólya's textbook [12] will be examined by means of Fujita's proligand method described in the present paper. Then, the results will be compared with those by Pólya et al. [12] in order to clarify merits of Fujita's proligand method.

5.2.1 Enumeration by Fujita's Proligand Method

Let us apply Theorems 2 to 4 to stereoisomer enumeration based on a prismane skeleton (**118**).

Example 6. The six positions of a prismane skeleton (**118**) are sequentially numbered as shown in Fig. 21. They construct a six-membered orbit governed by the RCR $(\mathbf{C}_s\backslash)\mathbf{D}_{3h}$, which can be obtained algebraically or diagrammatically, as shown in Table 2. According to the cycle

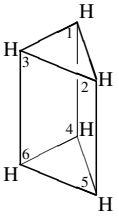

118

Figure 21: Prismane skeleton of $\mathbf{D}_{3h}$-symmetry.

Table 2: Right Coset Representation $(\mathbf{C}_s\backslash)\mathbf{D}_{3h}$ and Products of Sphericity Indices.[a]

symmetry operation		RCR $(\mathbf{C}_s\backslash)\mathbf{D}_{3h}$ as product of cycles	product of sphericity indices	product of dummy variables
I	$\sim$	$(1)(2)(3)(4)(5)(6)$	b_1^6	s_1^6
C_3	$\sim$	$(1\,2\,3)(4\,5\,6)$	b_3^2	s_3^2
C_3^2	$\sim$	$(1\,3\,2)(4\,6\,5)$	b_3^2	s_3^2
$C_{2(1)}$	$\sim$	$(1\,4)(2\,6)(3\,5)$	b_2^3	s_2^3
$C_{2(2)}$	$\sim$	$(1\,6)(2\,5)(3\,4)$	b_2^3	s_2^3
$C_{2(3)}$	$\sim$	$(1\,5)(2\,4)(3\,6)$	b_2^3	s_2^3
$\sigma_{d(1)}$	$\sim$	$\overline{(1)(2\,3)(3)(4)(5\,6)}$	$a_1^2c_2^2$	$s_1^2s_2^2$
$\sigma_{d(2)}$	$\sim$	$\overline{(1\,3)(2)(4\,6)(5)}$	$a_1^2c_2^2$	$s_1^2s_2^2$
$\sigma_{d(3)}$	$\sim$	$\overline{(1\,2)(3)(4\,5)(6)}$	$a_1^2c_2^2$	$s_1^2s_2^2$
σ_h	$\sim$	$\overline{(1\,4)(2\,5)(3\,6)}$	c_2^3	s_2^3
S_3	$\sim$	$\overline{(1\,5\,3\,4\,2\,6)}$	c_6	s_6
S_3^2	$\sim$	$\overline{(1\,6\,2\,4\,3\,5)}$	c_6	s_6

[a] Each cycle appearing in an improper rotation is designated by an overbar, which represents the inversion of ligand chirality.

structure of each permutation, the corresponding product of sphericity indices is calculated, as shown in Table 2. Hence, the CI-CF for this case is obtained by means of eq. 44 as follows:

$$\text{CI-CF}(\mathbf{D}_{3h},\$_d) = \frac{1}{12}\left(b_1^6+2b_3^2+3b_2^3+3a_1^2c_2^2+c_2^3+2c_6\right). \tag{79}$$

A set of six proligands is selected from **X** shown in eq. 47 (Example 1). The partition $[\theta]$ (eq. 30) for this case is calculated to be

$$[\theta] : h+x+p+\overline{p} = 6, \tag{80}$$

where the letters in the right-hand side represent non-negative integers. The molecular formula W_θ (eq. 49 or eq. 50) calculated by eq. 31 or eq. 32 is used on condition that the partition $[\theta]$ shown in eq. 80 is employed.

As for the ligand inventories (eqs. 39, 40, and 41), the same ligand inventories as eqs. 51–53 can be also used in this case. According to Theorem 2, the inventories (eqs. 51–53) are introduced into the CI-CF (eq. 79) to give the following generating function:

$$
\begin{aligned}
\sum_{[\theta]} B_\theta W_\theta \;=\;& (H^6+X^6)+(H^5X+HX^5)+(3H^4X^2+3H^2X^4)+3H^3X^3 \\
&+\frac{1}{2}(H^5p+H^5\overline{p})+\frac{1}{2}(X^5p+X^5\overline{p}) \\
&+5\times\frac{1}{2}(H^4Xp+H^4X\overline{p})+5\times\frac{1}{2}(HX^4p+HX^4\overline{p}) \\
&+10\times\frac{1}{2}(H^3X^2p+H^3X^2\overline{p})+10\times\frac{1}{2}(H^2X^3p+H^2X^3\overline{p}) \\
&+4\times\frac{1}{2}(H^4p^2+H^4\overline{p}^2)+4\times\frac{1}{2}(X^4p^2+X^4\overline{p}^2)+ \\
&+10\times\frac{1}{2}(H^3Xp^2+H^3X\overline{p}^2)+10\times\frac{1}{2}(HX^3p^2+HX^3\overline{p}^2) \\
&+9\times\frac{1}{2}(H^2X^2p^2+H^2X^2\overline{p}^2) \\
&+(4H^4p\overline{p}+4X^4p\overline{p})+(12H^3Xp\overline{p}+12HX^3p\overline{p})+18H^2X^2p\overline{p} \\
&+4\times\frac{1}{2}(H^3p^3+H^3\overline{p}^3)+4\times\frac{1}{2}(X^3p^3+X\,3\overline{p}^3) \\
&+10\times\frac{1}{2}(H^2Xp^3+H^2X\overline{p}^3)+10\times\frac{1}{2}(HX^2p^3+HX^2\overline{p}^3) \\
&+10\times\frac{1}{2}(H^3p^2\overline{p}+H^3p\overline{p}^2)+10\times\frac{1}{2}(X^3p^2\overline{p}+X^3p\overline{p}^2) \\
&+30\times\frac{1}{2}(H^2Xp^2\overline{p}+H^2Xp\overline{p}^2)+30\times\frac{1}{2}(HX^2p^2\overline{p}+HX^2p\overline{p}^2) \\
&+10\times\frac{1}{2}(H^2p^3\overline{p}+H^2p\overline{p}^3)+10\times\frac{1}{2}(X^2p^3\overline{p}+X^2p\overline{p}^3)+ \\
&+20\times\frac{1}{2}(HXp^3\overline{p}+HXp\overline{p}^3) \\
&+4\times\frac{1}{2}(H^2p^4+H^2\overline{p}^4)+4\times\frac{1}{2}(X^2p^4+X^2\overline{p}^4) \\
&+5\times\frac{1}{2}(HXp^4+HX\overline{p}^4) \\
&+(11H^2p^2\overline{p}^2+11X^2p^2\overline{p}^2)+17HXp^2\overline{p}^2 \\
&+\frac{1}{2}(Hp^5+H\overline{p}^5)+\frac{1}{2}(Xp^5+X\overline{p}^5) \\
&+5\times\frac{1}{2}(Hp^4\overline{p}+Hp\overline{p}^4)+5\times\frac{1}{2}(Xp^4\overline{p}+Xp\overline{p}^4) \\
&+10\times\frac{1}{2}(Hp^3\overline{p}^2+Hp^2\overline{p}^3)+10\times\frac{1}{2}(Xp^3\overline{p}^2+Xp^2\overline{p}^3) \\
&+\frac{1}{2}(p^6+\overline{p}^6)+\frac{1}{2}(p^5\overline{p}+p\overline{p}^5)+4\times\frac{1}{2}(p^4\overline{p}^2+p^2\overline{p}^4)+3p^3\overline{p}^3. \qquad (81)
\end{aligned}
$$

The coefficient of each term (or each combined term) represents the total number of stereoisomers with the corresponding weight (molecular formula).

To apply eq. 64 to the enumeration of achiral prismane derivatives, we start from the data for the improper rotations collected in Table 2. Thereby, the CI-CF$_A$ for this case is obtained as

follows:

$$\text{CI-CF}_A(\overline{\mathbf{D}}_{3h},\$_d) = \frac{1}{6}\left(3a_1^2c_2^2 + c_2^3 + 2c_6\right). \tag{82}$$

According to Theorem 3, the inventories (eqs. 51–53) are introduced into the CI-CF$_A$ (eq. 82) to give the following generating function:

$$\begin{aligned}\sum_{[\theta]} A_\theta W_\theta \;=\;& (\mathrm{H}^6+\mathrm{X}^6)+(\mathrm{H}^5\mathrm{X}+\mathrm{H}\mathrm{X}^5)+(2\mathrm{H}^4\mathrm{X}^2+2\mathrm{H}^2\mathrm{X}^4)+2\mathrm{H}^3\mathrm{X}^3\\ &+(3\mathrm{H}^4\mathrm{p}\overline{\mathrm{p}}+3\mathrm{X}^4\mathrm{p}\overline{\mathrm{p}})+(4\mathrm{H}^3\mathrm{X}\mathrm{p}\overline{\mathrm{p}}+4\mathrm{H}\mathrm{X}^3\mathrm{p}\overline{\mathrm{p}})+6\mathrm{H}^2\mathrm{X}^2\mathrm{p}\overline{\mathrm{p}}\\ &+(4\mathrm{H}^2\mathrm{p}^2\overline{\mathrm{p}}^2+4\mathrm{X}^2\mathrm{p}^2\overline{\mathrm{p}}^2)+4\mathrm{H}\mathrm{X}\mathrm{p}^2\overline{\mathrm{p}}^2\\ &+2\mathrm{p}^3\overline{\mathrm{p}}^3.\end{aligned} \tag{83}$$

By starting from the data collected in Table 2, eq. 70 is applied to the enumeration of enantiomeric pairs for chiral prismane derivatives. Thereby, the CI-CF$_C$ for this case is obtained as follows:

$$\text{CI-CF}_C(\mathbf{D}_{3h},\$_d) = \frac{1}{12}\left(b_1^6+2b_3^2+3b_2^3-3a_1^2c_2^2-c_2^3-2c_6\right). \tag{84}$$

where the plus sign of the term for each improper rotation in eq. 79 is changed into minus.

According to Theorem 4, the inventories (eqs. 51–53) are introduced into the CI-CF$_C$ (eq. 84) to give the following generating function:

$$\begin{aligned}\sum_{[\theta]} C_\theta W_\theta \;=\;& (\mathrm{H}^4\mathrm{X}^2+\mathrm{H}^2\mathrm{X}^4)+\mathrm{H}^3\mathrm{X}^3\\ &+\frac{1}{2}(\mathrm{H}^5\mathrm{p}+\mathrm{H}^5\overline{\mathrm{p}})+\frac{1}{2}(\mathrm{X}^5\mathrm{p}+\mathrm{X}^5\overline{\mathrm{p}})\\ &+5\times\frac{1}{2}(\mathrm{H}^4\mathrm{X}\mathrm{p}+\mathrm{H}^4\mathrm{X}\overline{\mathrm{p}})+5\times\frac{1}{2}(\mathrm{H}\mathrm{X}^4\mathrm{p}+\mathrm{H}\mathrm{X}^4\overline{\mathrm{p}})\\ &+10\times\frac{1}{2}(\mathrm{H}^3\mathrm{X}^2\mathrm{p}+\mathrm{H}^3\mathrm{X}^2\overline{\mathrm{p}})+10\times\frac{1}{2}(\mathrm{H}^2\mathrm{X}^3\mathrm{p}+\mathrm{H}^2\mathrm{X}^3\overline{\mathrm{p}})\\ &+4\times\frac{1}{2}(\mathrm{H}^4\mathrm{p}^2+\mathrm{H}^4\overline{\mathrm{p}}^2)+4\times\frac{1}{2}(\mathrm{X}^4\mathrm{p}^2+\mathrm{X}^4\overline{\mathrm{p}}^2)+\\ &+10\times\frac{1}{2}(\mathrm{H}^3\mathrm{X}\mathrm{p}^2+\mathrm{H}^3\mathrm{X}\overline{\mathrm{p}}^2)+10\times\frac{1}{2}(\mathrm{H}\mathrm{X}^3\mathrm{p}^2+\mathrm{H}\mathrm{X}^3\overline{\mathrm{p}}^2)\\ &+9\times\frac{1}{2}(\mathrm{H}^2\mathrm{X}^2\mathrm{p}^2+\mathrm{H}^2\mathrm{X}^2\overline{\mathrm{p}}^2)\\ &+(\mathrm{H}^4\mathrm{p}\overline{\mathrm{p}}+\mathrm{X}^4\mathrm{p}\overline{\mathrm{p}})+(8\mathrm{H}^3\mathrm{X}\mathrm{p}\overline{\mathrm{p}}+8\mathrm{H}\mathrm{X}^3\mathrm{p}\overline{\mathrm{p}})+12\mathrm{H}^2\mathrm{X}^2\mathrm{p}\overline{\mathrm{p}}\\ &+4\times\frac{1}{2}(\mathrm{H}^3\mathrm{p}^3+\mathrm{H}^3\overline{\mathrm{p}}^3)+4\times\frac{1}{2}(\mathrm{X}^3\mathrm{p}^3+\mathrm{X}\ 3\overline{\mathrm{p}}^3)\\ &+10\times\frac{1}{2}(\mathrm{H}^2\mathrm{X}\mathrm{p}^3+\mathrm{H}^2\mathrm{X}\overline{\mathrm{p}}^3)+10\times\frac{1}{2}(\mathrm{H}\mathrm{X}^2\mathrm{p}^3+\mathrm{H}\mathrm{X}^2\overline{\mathrm{p}}^3)\\ &+10\times\frac{1}{2}(\mathrm{H}^3\mathrm{p}^2\overline{\mathrm{p}}+\mathrm{H}^3\mathrm{p}\overline{\mathrm{p}}^2)+10\times\frac{1}{2}(\mathrm{X}^3\mathrm{p}^2\overline{\mathrm{p}}+\mathrm{X}^3\mathrm{p}\overline{\mathrm{p}}^2)\\ &+30\times\frac{1}{2}(\mathrm{H}^2\mathrm{X}\mathrm{p}^2\overline{\mathrm{p}}+\mathrm{H}^2\mathrm{X}\mathrm{p}\overline{\mathrm{p}}^2)+30\times\frac{1}{2}(\mathrm{H}\mathrm{X}^2\mathrm{p}^2\overline{\mathrm{p}}+\mathrm{H}\mathrm{X}^2\mathrm{p}\overline{\mathrm{p}}^2)\\ &+10\times\frac{1}{2}(\mathrm{H}^2\mathrm{p}^3\overline{\mathrm{p}}+\mathrm{H}^2\mathrm{p}\overline{\mathrm{p}}^3)+10\times\frac{1}{2}(\mathrm{X}^2\mathrm{p}^3\overline{\mathrm{p}}+\mathrm{X}^2\mathrm{p}\overline{\mathrm{p}}^3)+\\ &+20\times\frac{1}{2}(\mathrm{H}\mathrm{X}\mathrm{p}^3\overline{\mathrm{p}}+\mathrm{H}\mathrm{X}\mathrm{p}\overline{\mathrm{p}}^3)\end{aligned}$$

$$
\begin{aligned}
&+4\times\frac{1}{2}(H^2p^4+H^2\overline{p}^4)+4\times\frac{1}{2}(X^2p^4+X^2\overline{p}^4)\\
&+5\times\frac{1}{2}(HXp^4+HX\overline{p}^4)\\
&+(7H^2p^2\overline{p}^2+7X^2p^2\overline{p}^2)+13HXp^2\overline{p}^2\\
&+\frac{1}{2}(Hp^5+H\overline{p}^5)+\frac{1}{2}(Xp^5+X\overline{p}^5)\\
&+5\times\frac{1}{2}(Hp^4\overline{p}+Hp\overline{p}^4)+5\times\frac{1}{2}(Xp^4\overline{p}+Xp\overline{p}^4)\\
&+10\times\frac{1}{2}(Hp^3\overline{p}^2+Hp^2\overline{p}^3)+10\times\frac{1}{2}(Xp^3\overline{p}^2+Xp^2\overline{p}^3)\\
&+\frac{1}{2}(p^6+\overline{p}^6)+\frac{1}{2}(p^5\overline{p}+p\overline{p}^5)+4\times\frac{1}{2}(p^4\overline{p}^2+p^2\overline{p}^4)+p^3\overline{p}^3. \qquad (85)
\end{aligned}
$$

To testify the validity of the results shown in the generating functions (eqs. 81, 83, and 85), let us examine the coefficients of the term $H^4p\overline{p}$. The coefficient 4 of the term $H^4p\overline{p}$ in eq. 81 shows the existence of four stereoisomers, as shown in Fig. 22. Among them, three stereoisomers, i.e., **119**, **120**, and **121**, are achiral because of the coefficient 3 of the term $H^4p\overline{p}$ in eq. 83. The coefficient 1 of the term $H^4p\overline{p}$ in eq. 85 indicates one pair of enantiomers, i.e., **122/$\overline{\mathbf{122}}$**.

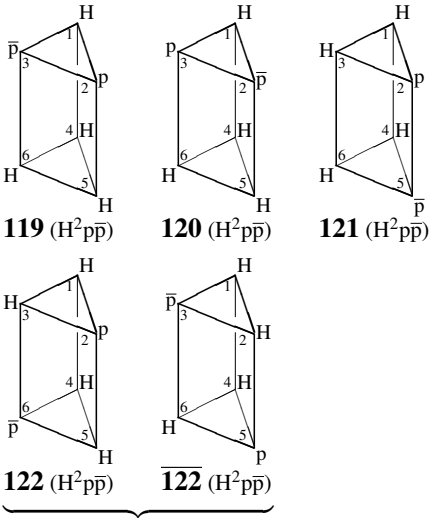

Figure 22: Three achiral stereoisomers and one pair of enantiomers which have the molecular formula $H^2p\overline{p}$.

The relationship between **119** and **120** is similar to a pseudoasymmetric case based on a tetrahedral skeleton (e.g., two achiral diastereomers of $HXp\overline{p}$). On the other hand, the achirality of **121** can be explained by regarding **121** as a kind of *meso*-compound. □

5.2.2 Enumeration by Pólya's Theorem

The enumeration of prismane derivatives by Pólya et al. [12] employed Pólya's theorem on condition that substituents were implicitly limited to atoms (or achiral ligands). Let us here examine whether Pólya's theorem works well or not if chiral ligands are permitted along with achiral ones (or atoms).

Example 7. The enumeration problem discussed in Example 6 is here solved by using Pólya's theorem. A Pólya's CI for enumerating prismane derivatives is cited from Chapter 6 of the Pólya's textbook [12]:

$$\mathrm{CI}(\mathbf{D}_3, s_d) = \frac{1}{6}\left(s_1^6 + 2s_3^2 + 3s_2^3\right), \tag{86}$$

which is obtained by collecting the dummy variables for the proper rotations ($\mathbf{D}_3$) from the data shown in Table 2. Because the inventory (eq. 75) can be also used in this case, it is introduced into the CI (eq. 86) to give the following generating function:

$$\begin{aligned}
f_{\mathbf{D}_3} \;=\;& (\mathrm{H}^6+\mathrm{X}^6)+(\mathrm{H}^5\mathrm{X}+\mathrm{H}\mathrm{X}^5)+(4\mathrm{H}^4\mathrm{X}^2+4\mathrm{H}^2\mathrm{X}^4)+4\mathrm{H}^3\mathrm{X}^3 \\
&+(\mathrm{H}^5\mathrm{p}+\mathrm{H}^5\overline{\mathrm{p}})+(\mathrm{X}^5\mathrm{p}+\mathrm{X}^5\overline{\mathrm{p}}) \\
&+(5\mathrm{H}^4\mathrm{X}\mathrm{p}+5\mathrm{H}^4\mathrm{X}\overline{\mathrm{p}})+(5\mathrm{H}\mathrm{X}^4\mathrm{p}+5\mathrm{H}\mathrm{X}^4\overline{\mathrm{p}}) \\
&+(10\mathrm{H}^3\mathrm{X}^2\mathrm{p}+10\mathrm{H}^3\mathrm{X}^2\overline{\mathrm{p}})+(10\mathrm{H}^2\mathrm{X}^3\mathrm{p}+10\mathrm{H}^2\mathrm{X}^3\overline{\mathrm{p}}) \\
&+(4\mathrm{H}^4\mathrm{p}^2+4\mathrm{H}^4\overline{\mathrm{p}}^2)+(4\mathrm{X}^4\mathrm{p}^2+4\mathrm{X}^4\overline{\mathrm{p}}^2)+ \\
&+(10\mathrm{H}^3\mathrm{X}\mathrm{p}^2+10\mathrm{H}^3\mathrm{X}\overline{\mathrm{p}}^2)+(10\mathrm{H}\mathrm{X}^3\mathrm{p}^2+10\mathrm{H}\mathrm{X}^3\overline{\mathrm{p}}^2) \\
&+(18\mathrm{H}^2\mathrm{X}^2\mathrm{p}^2+18\mathrm{H}^2\mathrm{X}^2\overline{\mathrm{p}}^2) \\
&+(5\mathrm{H}^4\mathrm{p}\overline{\mathrm{p}}+5\mathrm{X}^4\mathrm{p}\overline{\mathrm{p}})+(20\mathrm{H}^3\mathrm{X}\mathrm{p}\overline{\mathrm{p}}+20\mathrm{H}\mathrm{X}^3\mathrm{p}\overline{\mathrm{p}})+30\mathrm{H}^2\mathrm{X}^2\mathrm{p}\overline{\mathrm{p}} \\
&+(4\mathrm{H}^3\mathrm{p}^3+4\mathrm{H}^3\overline{\mathrm{p}}^3)+(4\mathrm{X}^3\mathrm{p}^3+4\mathrm{X}\,3\overline{\mathrm{p}}^3) \\
&+(10\mathrm{H}^2\mathrm{X}\mathrm{p}^3+10\mathrm{H}^2\mathrm{X}\overline{\mathrm{p}}^3)+(10\mathrm{H}\mathrm{X}^2\mathrm{p}^3+10\mathrm{H}\mathrm{X}^2\overline{\mathrm{p}}^3) \\
&+(10\mathrm{H}^3\mathrm{p}^2\overline{\mathrm{p}}+10\mathrm{H}^3\mathrm{p}\overline{\mathrm{p}}^2)+(10\mathrm{X}^3\mathrm{p}^2\overline{\mathrm{p}}+10\mathrm{X}^3\mathrm{p}\overline{\mathrm{p}}^2) \\
&+(30\mathrm{H}^2\mathrm{X}\mathrm{p}^2\overline{\mathrm{p}}+30\mathrm{H}^2\mathrm{X}\mathrm{p}\overline{\mathrm{p}}^2)+(30\mathrm{H}\mathrm{X}^2\mathrm{p}^2\overline{\mathrm{p}}+30\mathrm{H}\mathrm{X}^2\mathrm{p}\overline{\mathrm{p}}^2) \\
&+(10\mathrm{H}^2\mathrm{p}^3\overline{\mathrm{p}}+10\mathrm{H}^2\mathrm{p}\overline{\mathrm{p}}^3)+(10\mathrm{X}^2\mathrm{p}^3\overline{\mathrm{p}}+10\mathrm{X}^2\mathrm{p}\overline{\mathrm{p}}^3)+ \\
&+(20\mathrm{H}\mathrm{X}\mathrm{p}^3\overline{\mathrm{p}}+20\mathrm{H}\mathrm{X}\mathrm{p}\overline{\mathrm{p}}^3) \\
&+(4\mathrm{H}^2\mathrm{p}^4+4\mathrm{H}^2\overline{\mathrm{p}}^4)+(4\mathrm{X}^2\mathrm{p}^4+4\mathrm{X}^2\overline{\mathrm{p}}^4) \\
&+(5\mathrm{H}\mathrm{X}\mathrm{p}^4+5\mathrm{H}\mathrm{X}\overline{\mathrm{p}}^4) \\
&+(18\mathrm{H}^2\mathrm{p}^2\overline{\mathrm{p}}^2+18\mathrm{X}^2\mathrm{p}^2\overline{\mathrm{p}}^2)+30\mathrm{H}\mathrm{X}\mathrm{p}^2\overline{\mathrm{p}}^2 \\
&+(\mathrm{H}\mathrm{p}^5+\mathrm{H}\overline{\mathrm{p}}^5)+(\mathrm{X}\mathrm{p}^5+\mathrm{X}\overline{\mathrm{p}}^5) \\
&+(5\mathrm{H}\mathrm{p}^4\overline{\mathrm{p}}+5\mathrm{H}\mathrm{p}\overline{\mathrm{p}}^4)+(5\mathrm{X}\mathrm{p}^4\overline{\mathrm{p}}+5\mathrm{X}\mathrm{p}\overline{\mathrm{p}}^4) \\
&+(10\mathrm{H}\mathrm{p}^3\overline{\mathrm{p}}^2+10\mathrm{H}\mathrm{p}^2\overline{\mathrm{p}}^3)+(10\mathrm{X}\mathrm{p}^3\overline{\mathrm{p}}^2+10\mathrm{X}\mathrm{p}^2\overline{\mathrm{p}}^3) \\
&+(\mathrm{p}^6+\overline{\mathrm{p}}^6)+(\mathrm{p}^5\overline{\mathrm{p}}+\mathrm{p}\overline{\mathrm{p}}^5)+(4\mathrm{p}^4\overline{\mathrm{p}}^2+4\mathrm{p}^2\overline{\mathrm{p}}^4)+4\mathrm{p}^3\overline{\mathrm{p}}^3.
\end{aligned} \tag{87}$$

The coefficient of each term (or each combined term) represents the total number of stereoisomers with the corresponding weight (molecular formula).

Because this enumeration uses $\mathbf{D}_3$, each achiral stereoisomer is counted once and two enantiomers of each enantiomeric pair are counted separately. For example, the coefficient 5 of the term $\mathrm{H}^2\mathrm{p}\overline{\mathrm{p}}$ recognized that the five stereoisomers shown in Fig. 22 are counted separately. In other words, the achiralities of **119**, **120**, and **121** are not discriminated from the chiralities of **122** and $\overline{\mathbf{122}}$. □

Example 8. Another Pólya's CI for enumerating prismane derivatives is cited from Chapter 6 of the Pólya's textbook [12]:

$$\mathrm{CI}(\mathbf{D}_{3h}, s_d) = \frac{1}{12}\left(s_1^6 + 2s_3^2 + 4s_2^3 + 3s_1^2c_2^2 + 2s_6\right), \tag{88}$$

which is obtained by collecting all of the dummy variables for $\mathbf{D}_{3h}$ from the data shown in Table 2.

The inventory (eq. 75) is introduced into the CI (eq. 88) to give the following generating function:

$$\begin{aligned}
f_{\mathbf{D}_{3h}} \;=\; & (\mathrm{H}^6+\mathrm{X}^6)+(\mathrm{H}^5\mathrm{X}+\mathrm{H}\mathrm{X}^5)+(3\mathrm{H}^4\mathrm{X}^2+3\mathrm{H}^2\mathrm{X}^4)+3\mathrm{H}^3\mathrm{X}^3 \\
& +(\mathrm{H}^5\mathrm{p}+\mathrm{H}^5\overline{\mathrm{p}})+(\mathrm{X}^5\mathrm{p}+\mathrm{X}^5\overline{\mathrm{p}}) \\
& +(3\mathrm{H}^4\mathrm{X}\mathrm{p}+3\mathrm{H}^4\mathrm{X}\overline{\mathrm{p}})+(3\mathrm{H}\mathrm{X}^4\mathrm{p}+3\mathrm{H}\mathrm{X}^4\overline{\mathrm{p}}) \\
& +(6\mathrm{H}^3\mathrm{X}^2\mathrm{p}+6\mathrm{H}^3\mathrm{X}^2\overline{\mathrm{p}})+(6\mathrm{H}^2\mathrm{X}^3\mathrm{p}+6\mathrm{H}^2\mathrm{X}^3\overline{\mathrm{p}}) \\
& +(3\mathrm{H}^4\mathrm{p}^2+3\mathrm{H}^4\overline{\mathrm{p}}^2)+(3\mathrm{X}^4\mathrm{p}^2+3\mathrm{X}^4\overline{\mathrm{p}}^2)+ \\
& +(6\mathrm{H}^3\mathrm{X}\mathrm{p}^2+6\mathrm{H}^3\mathrm{X}\overline{\mathrm{p}}^2)+(6\mathrm{H}\mathrm{X}^3\mathrm{p}^2+6\mathrm{H}\mathrm{X}^3\overline{\mathrm{p}}^2) \\
& +(11\mathrm{H}^2\mathrm{X}^2\mathrm{p}^2+11\mathrm{H}^2\mathrm{X}^2\overline{\mathrm{p}}^2) \\
& +(3\mathrm{H}^4\mathrm{p}\overline{\mathrm{p}}+3\mathrm{X}^4\mathrm{p}\overline{\mathrm{p}})+(10\mathrm{H}^3\mathrm{X}\mathrm{p}\overline{\mathrm{p}}+10\mathrm{H}\mathrm{X}^3\mathrm{p}\overline{\mathrm{p}})+16\mathrm{H}^2\mathrm{X}^2\mathrm{p}\overline{\mathrm{p}} \\
& +(3\mathrm{H}^3\mathrm{p}^3+3\mathrm{H}^3\overline{\mathrm{p}}^3)+(3\mathrm{X}^3\mathrm{p}^3+3\mathrm{X}\,3\overline{\mathrm{p}}^3) \\
& +(6\mathrm{H}^2\mathrm{X}\mathrm{p}^3+6\mathrm{H}^2\mathrm{X}\overline{\mathrm{p}}^3)+(6\mathrm{H}\mathrm{X}^2\mathrm{p}^3+6\mathrm{H}\mathrm{X}^2\overline{\mathrm{p}}^3) \\
& +(6\mathrm{H}^3\mathrm{p}^2\overline{\mathrm{p}}+6\mathrm{H}^3\mathrm{p}\overline{\mathrm{p}}^2)+(6\mathrm{X}^3\mathrm{p}^2\overline{\mathrm{p}}+6\mathrm{X}^3\mathrm{p}\overline{\mathrm{p}}^2) \\
& +(16\mathrm{H}^2\mathrm{X}\mathrm{p}^2\overline{\mathrm{p}}+16\mathrm{H}^2\mathrm{X}\mathrm{p}\overline{\mathrm{p}}^2)+(16\mathrm{H}\mathrm{X}^2\mathrm{p}^2\overline{\mathrm{p}}+16\mathrm{H}\mathrm{X}^2\mathrm{p}\overline{\mathrm{p}}^2) \\
& +(6\mathrm{H}^2\mathrm{p}^3\overline{\mathrm{p}}+6\mathrm{H}^2\mathrm{p}\overline{\mathrm{p}}^3)+(6\mathrm{X}^2\mathrm{p}^3\overline{\mathrm{p}}+6\mathrm{X}^2\mathrm{p}\overline{\mathrm{p}}^3)+ \\
& +(10\mathrm{H}\mathrm{X}\mathrm{p}^3\overline{\mathrm{p}}+10\mathrm{H}\mathrm{X}\mathrm{p}\overline{\mathrm{p}}^3) \\
& +(3\mathrm{H}^2\mathrm{p}^4+3\mathrm{H}^2\overline{\mathrm{p}}^4)+(3\mathrm{X}^2\mathrm{p}^4+3\mathrm{X}^2\overline{\mathrm{p}}^4) \\
& +(4\mathrm{H}\mathrm{X}\mathrm{p}^4+4\mathrm{H}\mathrm{X}\overline{\mathrm{p}}^4) \\
& +(11\mathrm{H}^2\mathrm{p}^2\overline{\mathrm{p}}^2+11\mathrm{X}^2\mathrm{p}^2\overline{\mathrm{p}}^2)+16\mathrm{H}\mathrm{X}\mathrm{p}^2\overline{\mathrm{p}}^2 \\
& +(\mathrm{H}\mathrm{p}^5+\mathrm{H}\overline{\mathrm{p}}^5)+(\mathrm{X}\mathrm{p}^5+\mathrm{X}\overline{\mathrm{p}}^5) \\
& +(3\mathrm{H}\mathrm{p}^4\overline{\mathrm{p}}+3\mathrm{H}\mathrm{p}\overline{\mathrm{p}}^4)+(3\mathrm{X}\mathrm{p}^4\overline{\mathrm{p}}+3\mathrm{X}\mathrm{p}\overline{\mathrm{p}}^4) \\
& +(6\mathrm{H}\mathrm{p}^3\overline{\mathrm{p}}^2+6\mathrm{H}\mathrm{p}^2\overline{\mathrm{p}}^3)+(6\mathrm{X}\mathrm{p}^3\overline{\mathrm{p}}^2+6\mathrm{X}\mathrm{p}^2\overline{\mathrm{p}}^3) \\
& +(\mathrm{p}^6+\overline{\mathrm{p}}^6)+(\mathrm{p}^5\overline{\mathrm{p}}+\mathrm{p}\overline{\mathrm{p}}^5)+(3\mathrm{p}^4\overline{\mathrm{p}}^2+3\mathrm{p}^2\overline{\mathrm{p}}^4)+3\mathrm{p}^3\overline{\mathrm{p}}^3.
\end{aligned} \tag{89}$$

Let us examine the coefficient 3 of the term $\mathrm{H}^4\mathrm{p}\overline{\mathrm{p}}$ in eq. 89. In the condition of this enumeration under $\mathbf{D}_{3h}$, the five stereoisomers shown in Fig. 22 are categorized into three types, i.e., one pair of diastereomers **119/120**, one achiral stereoisomer **121**, and one pair of enantiomers **122/$\overline{\mathbf{122}}$**, which are distinctly counted to give 3 as the number of stereoisomers. This means that the diastereomeric relationship (**119/120**) is not discriminated from the enantiomeric relationship (**122/$\overline{\mathbf{122}}$**). □

5.3 Pólya's Theorem as a Special Case

As found easily, Pólya's Theorem is a special case of Theorem 2, where the sphericity indices a_d, b_d, and c_d are not discriminated so as to coalesce into the dummy variable s_d of one kind.

For example, the Pólya's CI shown in eq. 77 can be derived from the CI-CF shown in eq. 46 and the Pólya's CI shown in eq. 88 can be derived from eq. 79. Obviously, such Pólya's CIs lose the information on sphericities, which is carried by the corresponding CI-CFs.

Examples 4, 5, 7, and 8 have exhibited the scope and limitations of Pólya's theorem, which can be generalized as guiding principles for the usage of Pólya's theorem in stereoisomer enumeration. In order to obtain results consistent to stereochemistry, Pólya's theorem should be used under either one of the following conditions:

1. If both chiral ligands and achiral ligands are taken into consideration in stereoisomer enumeration based on a given skeleton of **G**-symmetry, a maximum chiral group of the **G** should be used in Pólya's theorem, even though the skeleton of **G**-symmetry is achiral. For example, the CIs shown in eq. 74 for allene derivatives and in eq. 86 for prismane derivatives should be used in place of eq. 77 and eq. 88. It should be noted however that the enumeration results disregard the chirality/achirality of each derivative and any enantiomeric relationships.

2. If the achiral group **G** of the given skeleton is adopted in Pólya's theorem, only achiral ligands (or atoms) should be taken into consideration. When the CIs shown in eq. 77 for allene derivatives and in eq. 88 for prismane derivatives are adopted, for example, only achiral ligands (or atoms) should be adopted as substituents. Otherwise, pseudoasymmetry cannot be treated properly, as exemplified in Examples 5 and 8.

These two restrictive conditions have never been pointed out, because stereochemical effects of inner structure (i.e., the chirality/achirality of ligands) have not been fully comprehended in chemical combinatorics based on Pólya's theorem. In fact, the conventional way for enumerating stereoisomers by Pólya's theorem (e.g., [12]) has implicitly adopted a narrower condition that substituents are limited to atoms (or achiral ligands) even whether the group **G** to be selected is regarded as being achiral or chiral.

5.4 Merits of Fujita's Proligand Method

Fujita's proligand method formulated newly by Theorem 2 has a merit of getting rid of the restrictive conditions due to Pólya's theorem. The stereochemical effects of inner structure (i.e., the chirality/achirality of ligands) are introduced into chemical combinatorics in terms of the sphericities of cycles. Thereby, enumeration results consistent to stereochemistry can be obtained even when both chiral ligands and achiral ligands are taken into consideration.

Moreover, Theorem 3 allows us to enumerate achiral stereoisomers; and Theorem 4 provides us with a tool for giving the number of enantiomeric pairs of chiral stereoisomers. As found in Examples 1–3, enumerated stereoisomers are categorized in terms of chirality/achirality, where pairs of enantiomers are recognized clearly. By combining results obtained by Theorems 2–3, troublesome situations due to *meso*-compounds and pseudoasymmetry can be solved succinctly.

Stereochemically speaking, Pólya's theorem may claim its validity and versatility by adopting the restrictive conditions described in Subsection 5.3. However, Pólya's corona [5, 6] as an extension of Pólya's theorem cannot remain within the restrictive conditions, because Pólya's corona inevitably treats inner structure in a nested fashion. In fact, Pólya's corona is incapable of treating cases in which chiral ligands appear as inner structure in a nested fashion, as pointed out recently [16]. Such problems as rejecting solution by Pólya's corona can be solved

by Fujita's proligand method, which has been provided in terms of the original formulation [15, 16, 17] as well as the present alternative formulation based on the concept of mandalas.

It should be emphasized that the concept of mandalas provides us with diagrammatical tools for realizing systematic approaches to Fujita's USCI approach (Parts 1 to 3) as well as to Fujita's proligand method (the present Part 4).

6 Conclusions

The concept of mandalas proposed in Part 2 of this series [2] has been used to give an alternative formulation of Fujita's proligand method, which was originally formulated by using the symmetrical properties of cyclic subgroups [15, 16, 17]. Thus, right and left coset decompositions have been formulated to give reference numbering and its inverse to the vertices of a regular body of **G**-symmetry (Part 1). After discussions on segmentation and subduction of regular bodies, the concept of mandalas proposed in Part 2 has been developed in terms of achiral assemblage and chiral assemblage, where a set of assemblies of **K**-symmetry is governed by the left coset representation **G**(/**K**). Each **K**-assembled mandala has been clarified to correspond to one stereoisomer of **K**-symmetry, i.e., an achiral molecule or a pair of enantiomers. The number of fixed assemblies per stereoisomer and the number of fixed assemblies per permutation have been compared to formulate Fujita's proligand method in an alternative way other than original formulation reported elsewhere [15, 16, 17]. Thereby, the number of achiral plus chiral stereoisomers, that of achiral stereoisomers, and that of chiral stereoisomers can be obtained distinctly. Deficiency of Pólya's theorem in stereoisomer enumeration and merits of Fujita's proligand method have been demonstrated by using allenes and prismanes as examples.

References

[1] Fujita, S. (2005) *MATCH Commun. Math. Comput. Chem.* **54**, 251–300.

[2] Fujita, S. (2006) *MATCH Commun. Math. Comput. Chem.* **55**, 5–38.

[3] Fujita, S. (2006) *MATCH Commun. Math. Comput. Chem.* **55**, 237–270.

[4] Fujita, S. (1991) *Symmetry and Combinatorial Enumeration in Chemistry* (Springer-Verlag, Berlin-Heidelberg).

[5] Pólya, G. (1937) *Acta Math.* **68**, 145–254.

[6] Pólya, G. & Read, R. C. (1987) *Combinatorial Enumeration of Groups, Graphs, and Chemical Compounds* (Springer-Verlag, New York).

[7] Rouvray, D. H. (1974) *Chem. Soc. Rev.* **3**, 355–372.

[8] Balaban, A. T. eds. (1976) *Chemical Applications of Graph Theory* (Academic Press, London).

[9] Balasubramanian, K. (1985) *Chem. Rev.* **85**, 599–618.

[10] Fujita, S. (1990) *J. Math. Chem.* **5**, 99–120.

[11] Fujita, S. (1990) *J. Math. Chem.* **5**, 121–156.

[12] Pólya, G., Tarjan, R. E., & Woods, D. R. (1983) *Notes on Introductory Combinatorics* (Birkhäuser, Boston).

[13] Fujita, S. (2000) *J. Chem. Inf. Comput. Sci.* **40**, 1101–1112.

[14] Fujita, S. (2001) *J. Math. Chem.* **30**, 249–270.

[15] Fujita, S. (2005) *Theor. Chem. Acc.* **113**, 73–79.

[16] Fujita, S. (2005) *Theor. Chem. Acc.* **113**, 80–86.

[17] Fujita, S. (2006) *Theor. Chem. Acc.* **115**, 37–53.

[18] Fujita, S. (1995) *Theor. Chem. Acta* **91**, 291–314.

[19] Fujita, S. (1995) *Theor. Chem. Acta* **91**, 315–332.

[20] Fujita, S. (1998) *Bull. Chem. Soc. Jpn.* **71**, 1587–1596.

[21] Fujita, S. (1999) *Bull. Chem. Soc. Jpn.* **72**, 2409–2416.

[22] Liu, G. L. (1968) *Introduction to Combinatorial Mathematics* (McGraw Hill, New York).

[23] Berge, C. (1968) *Principes de Combinatoire* (Dunod, Paris).

[24] Taylor, W. J. (1943) *J. Chem. Phys.* **11**, 532.

[25] van't Hoff, J. H. (1874) *Archives Néerlandaises des Sciences exactes et naturelles* **9**, 445–454.

[26] van't Hoff, J. H. (1875) *La Chimie Dans L'Espace* (P. M. Bazendijk, Rotterdam).